Evolution of multimodal final user equilibrium considering public transport network design history

Mostafa Ameli, Jean Patrick Lebacque, Ludovic Leclercq

▶ **To cite this version:**

Mostafa Ameli, Jean Patrick Lebacque, Ludovic Leclercq. Evolution of multimodal final user equilibrium considering public transport network design history. Transportmetrica B: Transport Dynamics, 2022, 10 (1), pp 923-953. 10.1080/21680566.2021.1973610 . hal-03454882

HAL Id: hal-03454882
https://hal.science/hal-03454882

Submitted on 29 Nov 2021

HAL is a multi-disciplinary open access archive for the deposit and dissemination of scientific research documents, whether they are published or not. The documents may come from teaching and research institutions in France or abroad, or from public or private research centers.

L'archive ouverte pluridisciplinaire **HAL**, est destinée au dépôt et à la diffusion de documents scientifiques de niveau recherche, publiés ou non, émanant des établissements d'enseignement et de recherche français ou étrangers, des laboratoires publics ou privés.

TRANSPORTMETRICA B: TRANSPORT DYNAMICS

Evolution of multimodal final user equilibrium considering public transport network design history

Mostafa Ameli[a], Jean Patrick Lebacque[a] and Ludovic Leclercq[b]

[a]University Gustave Eiffel, COSYS, GRETTIA, Paris, France;
[b]University Gustave Eiffel, ENTPE, LICIT, F-69518, Lyon, France

ARTICLE HISTORY
Compiled March 8, 2021

Abstract
Analyzing the properties of a network equilibrium (uniqueness and stability) can help to have a better view about network state, robustness, and the effect of any variation in the network. In this study, we investigated the impacts of network design history on day-to-day multimodal user equilibrium. In particular, we investigate the long-term evolution of the network, including opening new multimodal options and its impacts on the final network equilibrium. First, the analysis focuses on static network loading with different successive configurations. This structure makes analytical derivations possible, highlighting the problem. Then, a more realistic setting is studied by simulation. A large-scale multimodal network with the flexible opening over time of three possible transport facilities shows that the final equilibrium is not unique; more importantly, significant differences can be observed in public transportation occupancy, while user equilibrium is enforced in all situations. Some solutions prove to be better from the collective viewpoint (shorter total travel time), thus giving new insight into public transport planning.

KEYWORDS
Multimodal; Uniqueness; Day-to-day; Dynamic traffic assignment; Projected dynamical system; Trip-based; Vector fields

1. Introduction

User Equilibrium (UE) is achieved when all users experience the minimum possible path cost given the network constraints and other users' path choices (Wardrop 1952). Unicity conditions for UE situation has been extensively studied in the literature for traffic assignment problems (Beckmann, McGuire, and Winsten (1956); Daganzo (1985); Mounce and Smith (2007)). Iryo (2015) defines the unicity of the UE solution as one of three situations: only a unique link flow value vector meets UE requirements, or the link travel time profiles of the UE solution are uniquely determined, and the solution set for the network equilibrium model is convex. Note that the convexity of the solution set guarantees the existence of an equilibrium (Iryo and Smith 2018). A key argument (sufficient condition) for unicity is a strictly monotone travel time function with respect to the number of travelers that use a path (Smith (1979); Aashtiani and Magnanti (1981); Florian and Hearn (1995)). This condition is quite restrictive as monotonicity can be guaranteed at the link level for mono-modal flow but hardly at

CONTACT Ludovic Leclercq. Email: ludovic.leclercq@univ-eiffel.fr

the path level because of the intersection functioning (Yang and Huang 2004). Traffic assignment models address the network equilibrium problem, including the travel time calculation, mathematically.

In brief, a traffic assignment model calculates the path flow distribution over possible paths for all OD pairs, considering the total demand and the network traffic conditions (Smith 1983). Traffic assignment models can be divided into two categories: flow-based and trip-based (Patriksson 2015). A flow-based traffic assignment is a continuous model, but in a trip-based approach, the path flow should correspond to integer values as all users are considered individually in the network and cannot be split. The flow-based approach is good for simplifying the problem, as it takes advantage of continuous models for analytical investigations. Here, we first investigate the problem analytically following a flow-based approach and then we address a real case numerically using a trip-based simulator.

The Static Traffic Assignment (STA) problem is defined when the system properties, e.g., Origin-Destination (OD) matrix and the link flows, are assumed to be time-independent. On the other hand, if time dependence is considered, the problem becomes a Dynamic Traffic Assignment (DTA). DTA is much more complicated than STA, both computationally and conceptually (Peeta and Ziliaskopoulos 2001).

Much research on the unicity of STA solutions has been performed with several assumptions and limitations on the traffic network model (Netter (1972); Dafermos (1982); Nagurney (1984); Wynter (2001); Wie, Tobin, and Carey (2002); Florian and Morosan (2014); Sun, Cheng, and Xu (2014)). For DTA models, the conditions of unicity have been appropriately reviewed by Iryo (2013). His review shows that almost all the studies address unicity in small and medium traffic networks by applying analytical approaches because in the large-scale DTA problem, evaluating the solution set is very complex and not feasible. This study takes a different angle, as we are interested in situations where unicity conditions do not hold. The reasons for multiple equilibria to occur in a dynamic traffic network are as follows:

- The link cost function, i.e., the bottleneck model vs. whole link model (Friesz et al. (2001); Lindsey (2004); Silva et al. (2016); Osawa, Fu, and Akamatsu (2018))
- The transportation mode cost function.
- The transportation mode interaction model (Jiang et al. 2016).
- The symmetry of the network, i.e., loopy network (Iryo 2011).
- Multi-class users (Marcotte and Wynter (2004); Konishi (2004); Nilsson, Grover, and Kalabić (2018)).

One very classical setting in which multiple equilibria can occur is the multimodal traffic assignment problem. In a multimodal urban transportation network, users have access to different modes, e.g., car, bus, and metro, which changes their characteristics when they swap from one mode to another (Corman, Viti, and Negenborn 2017). Therefore, according to the transportation mode cost function and the mode interaction model, the monotonicity condition simply does not hold (Mounce and Smith 2007) even at the link level. Besides, Iryo and Watling (2019) showed that the existence of multiple equilibria is common. He investigated the stability of the final equilibrium on a STA problem with two alternatives and two user groups and proved that the system could be converged to multiple equilibria. In such cases, the final equilibrium not only depends on the initial state but also on the convergence process. This study focuses on the second aspect.

To investigate the multiple equilibria problem with multimodal settings, we consider

a day-to-day convergence process. A fraction of users may update their path choice for the next day in the light of the traffic conditions that they experience during the current day (Ma, Xu, and Chen 2021). Users swap to a path with minimum travel time as they try to optimize their own gain (Mounce 2007). When unicity holds, this process converges to the single equilibrium loading (Zhao, Wan, and Bi 2018). Here, we focus on what happens when multiple solutions can be reached as we aim to highlight what may drive the system to one equilibrium rather than another. More specifically, when considering a long-term day-to-day process, the final network may not be built at once but results from the successive opening of additional facilities. In this paper, we consider that the road network is stable over the entire time horizon and that the public transport network is subject to the regular new openings (bus or metro lines). We define this opening process as the network history and investigate how it would affect the final equilibrium state of the network.

First, we perform an analytical investigation and demonstrate the existence of multiple equilibria with respect to the network history of day-to-day STA. Second, we address the same question through simulation for a more complex test case (large-scale network, dynamic traffic assignment, multiple configurations for the network history). The analytical study highlights the causes for the existence of multiple solutions and the influence of network history. The numerical study aims to provide results considering a realistic urban setting. The influence of network history is investigated with a different angle as we are more interested in the convergence of multiple equilibria, i.e., the description of the differences between final possible states. A specific finding is that several network history configurations lead to shorter total travel times for the system than others, and to different mode ratios in the system. This may be of interest when considering public transport planning.

2. Model and experiment design for multimodal STA

In this section, we perform an analytical exploration of the non-uniqueness of the network UE solution in a day-to-day multimodal framework. Netter (1972) was the first to study multiple equilibria for a bi-modal (car and bus) network loading for a two-arc network with linear cost functions. Wynter (2001) extended the study by designing a numerical example with polynomial cost functions on the same graph. Here, we focus on the impact of network design history on the final network state. The general idea is that the day-to-day process represents the way in which the users learn about the network state. Each day, a fraction of users adjust their paths to account for the travel times experienced the day before. Such a process converges to a stable solution, but it may differ depending on the initial state and the learning process. Introducing the possible options successively and in different orders results in the same final network layout but through different steps.

2.1. *Static test case*

Let us consider a network with two nodes ($N = \{O, D\}$) and three directed paths from O to D ($A = \{1, 2, 3\}$). There are three modes of transportation (set of modes: $M = \{C, B, T\}$) which are referred to as car, bus and train (metro) (figure 1). There are two bus lines between origin and destination. Paths 1 and 2 are shared between car and bus and path 3 is the train line. Therefore, there are five feasible path choices to reach the destination: car by path 1, car by path 2, bus line on path 1, bus line on

path 2, and train on path 3, figure 1.

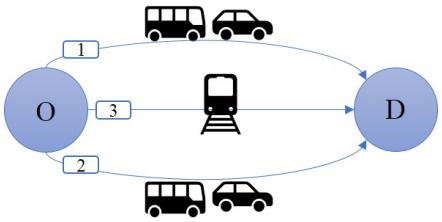

Figure 1. A network with a single OD pair, three paths and three transportation modes.

The notations are:

a: Index of path, $a \in A$.
m: Index of mode, $m \in M$.
M_{MV}: The set of motor vehicles (car and bus), $M_{MV} = \{C, B\}$
D^m: Demand of mode m.
c^m: Minimum cost for mode m.
c_a^m: Cost of path a for mode m.
f_a^m: Flow of mode m on path a.

Note that the total demand for public transportation D_{PT} and cars D^C are given. The demand for public transportation is disaggregated per mode:

$$D_{PT} = \sum_{m \in \{B,T\}} D^m \tag{1}$$

According to the definition, the total flow of each mode is:

$$D^m = \sum_a f_a^m; \quad \forall f_a^m \geq 0, m \in M_{MV} \tag{2}$$

$$D^T = f_3^T \tag{3}$$

The cost for path a and mode m not only depends on the path flow for this mode but also the path flow of other modes as all vehicles interact. For example, on paths 1 and 2, bus and car flows result from a global congestion level that influences both bus and cars travel costs.

$$c_a^m = g_a^m + \sum_{\mu \in M_{MV}} h_a^{m,\mu} f_a^\mu, \quad \forall m \in M_{MV}, a \in A \tag{4}$$

Here, we assume that c_a^m is defined as a linear function where g_a^m is the free flow cost of mode m on path a and $h_a^{m,\mu}$ is the impact factor of f_a^μ on the cost of mode m. Using linear functions may look as a strong assumption compared to more realistic polynomial or exponential shape, e.g., BPR function (Bureau of Public Roads 1964)

or considering path capacity constraints (Beckmann, McGuire, and Winsten 1956). It is not here as our main purpose is to understand the causes for multiple equilibria to appear. What triggers this phenomenon is the cross-dependency of the cost among modes, which is properly accounted here.

The cost function for path 3 is even much simpler. First only a train option is available, as the cost should only depends on the demand for train. Second, train service is only adjusted to the demand on the long run (every year or twice a year when a new timetable is proposed). So during the day-to-day STA process, the perceived cost by users is mainly fixed as a combinations of the travel time and the cost. In the end: $c_3^T = \lambda$, where λ is considered as a constant value.

According to the Wardrop equilibrium definition, the network is at the UE flow distribution if and only if:

$$\begin{cases} f_a^m (c_a^m - c^m) = 0, & \forall m \in M, a \in A \\ f_a^m f_a^\mu (c_a^m - c_a^\mu) = 0, & \forall m, \mu \in \{B, T\}, a \in A \end{cases} \tag{5}$$

Therefore, when the equilibrium is reached, the cost of all used paths of mode m is equal to c^m. The costs are assumed to be asymmetric: the effect of cars on buses is not the same as the effect of buses on cars. In other words, in the network (figure 1) for one or more modes $m_1 \neq m_2$:

$$\frac{\partial c_a^{m_1}}{\partial f_a^{m_2}} \neq \frac{\partial c_a^{m_2}}{\partial f_a^{m_1}} \iff h_a^{m_1,m_2} \neq h_a^{m_2,m_1} \quad \forall a = 1, 2, \ \forall m_1, m_2 = B, C \tag{6}$$

2.2. *Network history design*

Here, we are interested in investigating the equilibrium when intermediate changes in the network design occur. In other words, the final network layout is always the same, but it may result from different intermediate steps, see table 1. Scenario 1 has no train line at first place. Thus, an intermediate equilibrium state (UE) is first achieved through the day-to-day learning process before the train line is added. Then, the metro line is added, and the second convergence process proceeds. Scenario 2 assumes that there are only cars and trains, and no buses during the first convergence period. Then buses are added and a second convergence process is initiated starting from the equilibrium obtained by the first process. Scenario 3 is when all modes are active from the beginning. We will calculate the final network equilibrium for all the scenarios in table 1 and examine why different equilibrium may be raised.

3. Bi-modal equilibrium analysis: the car-bus case

3.1. *Cost-flow diagram for equilibrium calculation*

In order to calculate the intermediate equilibrium for Scenario 1, we first explore the non-uniqueness of the network without train ($D^T = 0$), i.e., we analyze the equilibrium solution(s) for the initial equilibrium state of scenario 1 in table 1. As mentioned before, the D^C and D_{PT} are fixed values and the inputs of the model. Let us express costs on paths 1 and 2 as functions of the flows f_1^m, for $m \in M_{MV}$. In view of equation 2, we

Table 1. The scenarios of network design for the mono-OD test case.

Scenario	Initial equilibrium state	Final state
1	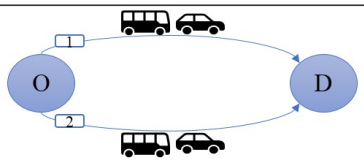	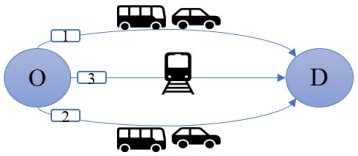
2	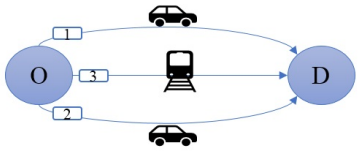	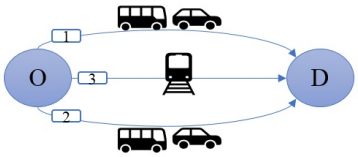
3	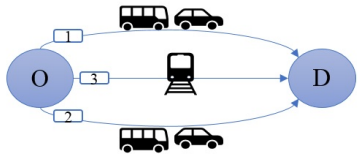	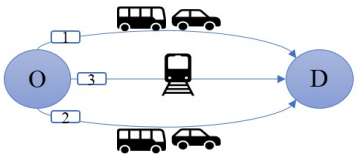

can consider $(f_1^m)_{m\in M_{MV}}$ as an independent and $(f_2^m)_{m\in M_{MV}}$ as a dependent variable. Therefore, the demand and cost functions are as follows:

$$D^B = D_{PT} \tag{7}$$

$$f_2^m = D^m - f_1^m, \quad \forall m \in M_{MV} \tag{8}$$

$$c_1^m = g_1^m + \sum_{\mu\in M_{MV}} h_1^{m,\mu} f_1^\mu, \quad \forall m \in M_{MV} \tag{9}$$

$$c_2^m = g_2^m + \sum_{\mu\in M_{MV}} h_2^{m,\mu} D^\mu - \sum_{\mu\in M_{MV}} h_2^{m,\mu} f_1^\mu, \quad \forall m \in M_{MV} \tag{10}$$

To avoid the repetition, we define $\bar{g}_2^m$:

$$\bar{g}_2^m = g_2^m + \sum_{\mu\in M_{MV}} h_2^{m,\mu} D^\mu, \quad \forall m \in M_{MV} \tag{11}$$

According to equation 6, on each path, the impacts of two modes on each other are not the same, which represents the real interaction between modes. In other words, the Jacobian matrix ($\nabla c(f)$) of the car and the bus cost functions is not symmetric positive definite ($c(f)$ is not the gradient of a convex function), which means the cost functions for path 1 and 2 are not monotonic (Iryo 2013; Yang and Huang 2005).

The network equilibrium state with two modes has two options for each path: the path is used in the equilibrium path flow distribution or not. In order to visualize the equilibrium point, we discuss the possibilities for path 1. Figure 2 presents the cost-flow diagram of the network based on path 1 and on the independent flows f_1^m (using equations 8 and 10).

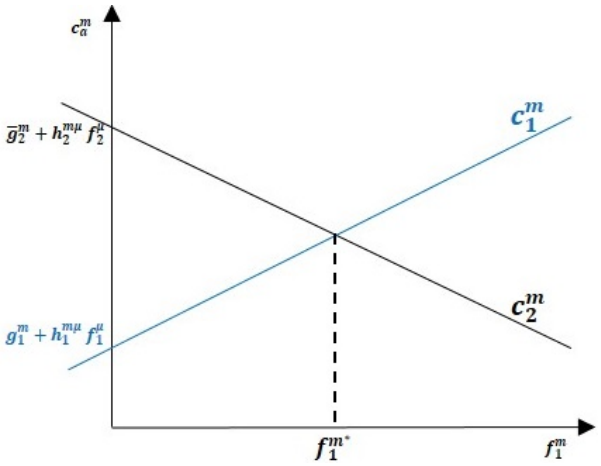

Figure 2. Cost-flow diagram based on path 1

If $c_1^m < c_2^m$, we need to increase f_1^m to reach equilibrium ($c_1^m = c_2^m$), thus we can show in the plane (f_1^C,f_1^B) the natural direction of variation for flows is $\Delta c^m = (c_2^m - c_1^m)_{m=1,2}$. According to figure 2 and equation 8 (when there is no train), we have to draw $\Delta c^m = c_2^m - c_1^m = 0$ based on the flow value of f_1^m to show the equilibrium point. The flows f_2^m can be considered dependent variables. Consequently, by equation 10 we can draw the curves $\Delta c^m = 0$ of the two vehicular modes on the flow diagram of path 1 in the (f_1^C,f_1^B) plane. The configuration of the diagram depends on the value of the $h_a^{m,\mu}$. In order to draw the two linear flow diagrams, we need at least three points if they have an intersection. The conditions are extracted from the possible common point:

$$\Delta c^m = c_2^m - c_1^m = \bar{g}_2^m - g_1^m - \sum_{\mu=1,2} (h_1^{m,\mu} + h_2^{m,\mu}) f_1^\mu = 0 \tag{12}$$

According to the equation 12, we can extract the slope of Δc^m diagram. The intersect of $\Delta c^m = 0$ with $f_1^B = 0$ is:

$$F_1^C(m) = (\bar{g}_2^m - g_1^m)/(h_1^{m,C} + h_2^{m,C}) \tag{13}$$

and the intersect with $f_1^C = 0$ is:

$$F_1^B(m) = (\bar{g}_2^m - g_1^m)/(h_1^{m,B} + h_2^{m,B}) \tag{14}$$

Therefore, the slope of $\Delta c^m = 0$ line for mode m on path 1 is as follows:

$$\frac{1}{(h_1^{m,B} + h_2^{m,B})} / \frac{1}{(h_1^{m,C} + h_2^{m,C})} = \rho_m = \frac{(h_1^{m,C} + h_2^{m,C})}{(h_1^{m,B} + h_2^{m,B})} \tag{15}$$

The diagram configuration depends on the values of ρ_m. We need to know the relation of the flow diagram's slope for mode B (ρ_B) in relation to the slope of the line Δc^C (ρ_C). Thus, with ρ_m we can conditionally draw the flow diagram of $\Delta c^m = 0$ for two modes on path 1. Before calculating the equilibrium and draw the figure for path 1, a day-to-day process in static case should be defined.

3.2. *The projected dynamical system of traffic assignment*

We define the network equilibrium problem as a projected dynamical system. It has been proved by several studies (see e.g.,Nagurney and Zhang (2012); Smith (1993); Huang and Lam (2002); Jin (2007); Lebacque, Ma, and Khoshyaran (2009)) that projected dynamical systems find the equilibrium point(s) by producing the solution trajectory (mapping function) based on a fixed point theory. Let K be the rectangle $[0, D^C] \times [0, D^B]$ of admissible flows based on the constraints 2. Let $\Delta c : \mathbb{R}^2 \mapsto \mathbb{R}^2$ be the vector field given by $\left(\Delta c^C, \Delta c^B\right)$ and let $f = \left(f_1^C, f_1^B\right)$ be the vector of independent path flows. Let $\Pi_K(f, .)$ denote the projector on the tangent cone of K at f. The projected dynamical system PDS$(f, \Delta c(f))$ is defined by:

$$\dot{f} = \Pi_K(f, \Delta c(f)) = \Pi_K^m(f_1^m, \Delta c^m(f)) = \lim_{t \downarrow 0} P_K[f_1^m + t(\Delta c^m(f))], \quad \forall m \in M_{MV} \tag{16}$$

Let $\Gamma^K(f) \overset{def}{=} \Pi_K(f, \Delta c(f))$ be the projection of the field $\Delta c(f))$ on K. The point f^* is an equilibrium point (i.e) satisfies equations (2), (4), and (5), if and only if $\Gamma^K(f^*)$ is equal to zero, which means that f^* is a fixed point of the projected dynamical system PDS$(f, \Delta c(f))$. Thus the field lines (trajectories) of Γ^K in the solution space can be used to describe the day-to-day STA learning process of travellers.

Figure 3 presents the flow diagram of path 1 depending on the respective values of ρ_B and ρ_C. The field lines indicate how the solution moves toward the equilibrium. They are determined by equation 16.

By definition, the network is at UE state where the result of the $\Gamma^K(f)$ is zero at the current point, which corresponds to a fixed point of the PDS$(f, \Delta c(f))$. This refers to the following conditions for the equilibrium solution based on Δc^m and the projected dynamical system (Nagurney and Zhang 2012):

$$\Pi_K^m(f^m, \Delta c^m(f)) = \begin{cases} P_+(\Delta c^m(f)) & \text{if } f^m = 0 \\ \Delta c^m(f) & \text{if } 0 < f^m < D^m \\ P_-(\Delta c^m(f)) & \text{if } f^m = D^m \end{cases}, \quad \forall m \in M_{MV} \tag{17}$$

where $P_+(g)$ and $P_-(g)$ are defined as follows:

$$P_+(g) \begin{cases} = 0 & ; g \geq 0 \\ \leq 0 & ; g \leq 0 \end{cases} \tag{18}$$

$$P_-(g) \begin{cases} = 0 & ; g \leq 0 \\ \geq 0 & ; g \geq 0 \end{cases} \tag{19}$$

We consider the stationary point as the stable equilibrium based on the definition in Iryo and Watling (2019). Therefore, the definition of the equilibrium point is different from the stationary point in this context. The stability of the solution can be analyzed based on the PDS($f, \Delta c(f)$). The unstable equilibrium may exist in the solution space, where the $\Delta c^m = 0$, but the PDS($f, \Delta c(f)$) of neighbor points lead the system to another equilibrium. In other words, the UE solution E is stable only if, the day-to-day process brings the solution back to E when a small perturbation ϵ moves it from E in any direction of the feasible region (converging arrows to E). By this definition, in figure 3(a), the intersection of the two diagrams is an unstable equilibrium (Unstable E), and the two other equilibria are stable (Stable E).

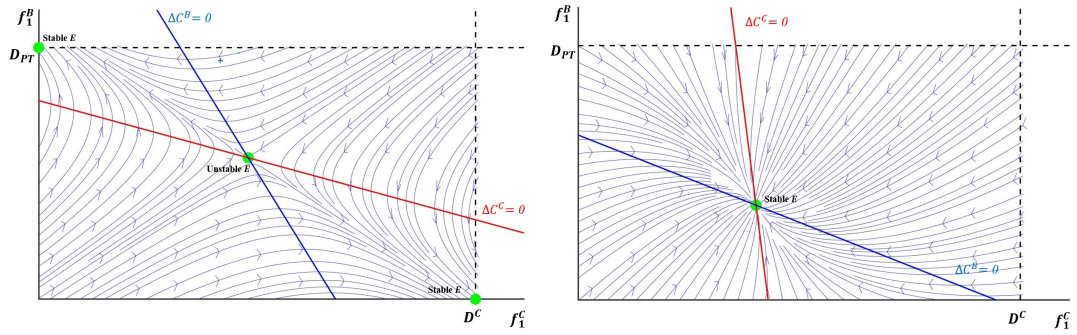

(a) $\rho_B > \rho_C$ (b) $\rho_B < \rho_C$

Figure 3. The equilibrium solution(s) on the flow diagram of path 1

At each point in figure 3 that does not locate at an equilibrium state, we can analyze the field line based on Δc^m. For instance, if $\Delta c^C > 0$, which means that the cost of the car on path 1 is lower than that on path 2, so a part of the flow of path 2 will be shifted to path 1, thus on the flow diagram of path 1, f_1^C increases and the network state moves to the right. In a similar manner, when $\Delta c^C < 0$, f_1^C decreases and the solution moves to the left. For Δc^B, if the flow of bus lines shifts from one path to another, according to equations 7 and 11, lines $f_1^B = D^B$ and $\Delta c^B = 0$ are moved. Therefore, if $\Delta c^B > 0$, as with the car, a part of f_2^B is swapped to path 1, which means f_1^B increases and the network state moves up. Finally, when $\Delta c^B < 0$, f_1^B decreases and the solution moves down. The field line is the results of both variables (Δc^C and Δc^B). Consequently, the day-to-day STA (PDS($f, \Delta c(f)$)) changes the state of the network until the UE is reached. For example, figure 4 presents the trajectory of the different starting points in the solution space. Almost all of the initial path flow distribution converges to the two stable equilibria on the corners while there is a rare situation wherein the starting point is located on a line whereon the field lines direction is thorough to the unstable equilibrium (the intersection of Δc^C and Δc^B).

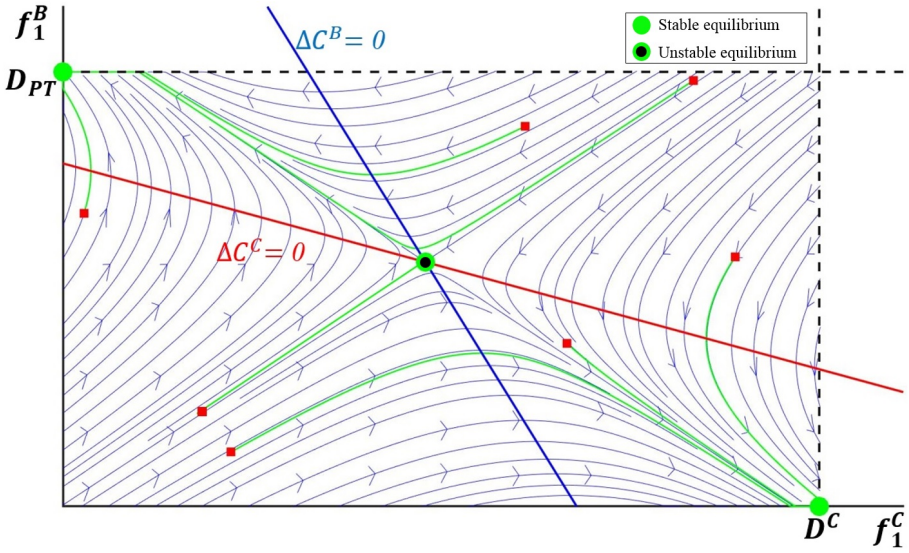

Figure 4. The trajectory of different initial solutions (red squares) on flow diagram of path 1

3.3. *Sufficient conditions for multiple equilibria*

$\rho_B > \rho_C$ means that the cross impacts of different modes are grater than self impacts of the mode. In other words according to equation 15:

$$(h_1^{B,C} + h_2^{B,C})(h_1^{C,B} + h_2^{C,B}) > (h_1^{B,B} + h_2^{B,B})(h_1^{C,C} + h_2^{C,C}) \tag{20}$$

This setting is more realistic because the production of the total impact coefficients of bus on car ($h_a^{C,B}$) and car on bus ($h_a^{B,C}$) is higher than the production of the total impact of car on car ($h_a^{C,C}$) and bus on bus ($h_a^{B,B}$).

If $\rho_B > \rho_C$, the flow diagram for this configuration is presented in figure 3(a). Based on the initial point, we have three possible equilibria. Figure 3(b) presents the flow diagram where $\rho_B < \rho_C$. This configuration leads to a unique stable solution at the intersection of two flow diagrams. Consequently, in the first configuration, we will have a conditional equilibrium based on the values of ρ_C, ρ_B.

$$\text{Solution set} = \begin{cases} \rho_B > \rho_C & \text{3 equilibria, 1 unstable and 2 stable,} \\ \rho_C > \rho_B & \text{1 equilibrium, stable.} \end{cases} \tag{21}$$

If we consider other configurations for $\rho_B > \rho_C$ where the two lines $\Delta c^C = 0$ and $\Delta c^B = 0$ do not intersect inside K, we will have a unique equilibrium. For instance, if the flow line for car ($m = C$) lies below the bus line ($m = B$), then there is an equilibrium which is stable with $f_1^B = D^B$ and $f_1^B = 0$. This configuration is shown in Figure 5(a). If the relation between the flow of two modes on Path 1 is inverse ($f_1^B = 0$), we will have a stable equilibrium according to figure 5(b). If we look at the configuration where two lines ($\Delta c^m = 0$) intersect (as in figures 3(a)), we do not necessarily obtain multiple solutions. If the intersection is outside the feasible solution set, we also obtain a unique solution. Figure 5(c) presents an example when we obtain a unique solution, and two diagrams intersect outside the feasible region (K).

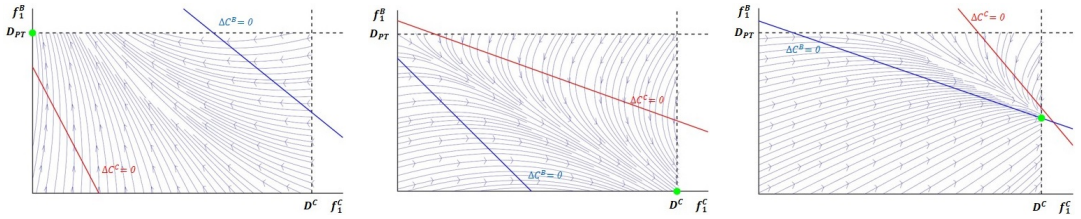

(a) $F_1^B = 0$ (b) $F_1^C = 0$ (c) $F_1^C = D^C$ and $F_2^C = 0$

Figure 5. The flow diagram of special cases for $\rho_B > \rho_C$ (The intersection is outside K)

Thus, in order to obtain multiple solutions, it is required that the lines $\Delta c^m = 0$ intersect inside K and that their slopes are such that the intersection point is unstable for the PDS$(f, \Delta c(f))$. Consequently, the sufficient conditions for multiple equilibria are:

$$\begin{cases} \rho_B > \rho_C \\ (\Delta c^C = 0) \cap (\Delta c^B = 0) \in K \end{cases} \tag{22}$$

where $(\Delta c^C = 0) \cap (\Delta c^B = 0)$ is obtained by solving $\Delta c^B = \Delta c^C = 0$ and depends on the value of D^C and D^B. Note that at some limited cases wherein $\Delta c^m = 0$ intersection is located on the border of K (feasible area), we get two equilibria: one stable and one unstable.

As mentioned before, we can further refine the general setting by introducing capacity constraints for each mode/path. This refer to only limits the feasible solution space. For instance, the path flow capacity for path a (Ω_a) can be defined as follows:

$$\Omega_a : \sum_{\mu \in M_{MV}} \omega_a^\mu f_a^\mu \leq \omega_a^{max} \tag{23}$$

where ω_a^μ denotes the weight factor for f_a^μ and ω_a^{max} denotes the maximum capacity of path a. Constraint 23 further reduces the feasible solution space. In order to draw the constraint on flow diagram, we need to extract the linear constraints from Constraint 23 by using equation 8:

$$\Omega_a = \begin{cases} f_1^B \leq \frac{1}{\omega_1^B}(\omega_1^{max} - \omega_1^C f_1^C) \\ f_1^B \geq D_{PT} - \frac{1}{\omega_2^B}(\omega_1^{max} - \omega_2^C (D^C - f_1^C)) \end{cases} \tag{24}$$

These constraints may impact on the final equilibrium solution. Figure 6 presents the solution space with constraints. In figure 6(a), constraints do not change the equilibria, while in figure 6(b) the equilibrium points are updated with respect to the constraints. The constraints can also eliminate equilibrium point(s) in feasible solution space (figure 6(c)). This analysis shows that capacity constraints do not fundamentally change the problem but may only restrict the number of possible equilibria. In the sequel, we come back to the original settings with infinite capacity in order to explore the convergence problem with multiple steps related to the network history.

Here, we proved that even with two modes car and bus, we have multiple equilibria.

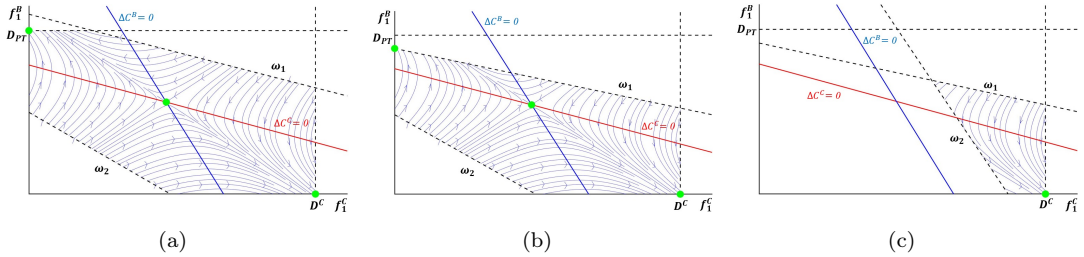

Figure 6. The flow diagram of the system with capacity constraints.

The final equilibrium is defined by the initial network state before the learning process starts. In our test case, we can divide the solution space into two regions wherein all the points are converged to a stable equilibrium. Figure 7 presents these two regions on the cost-flow diagram. If the initial network state is located in the blue area, the system will converge to the stable equilibrium on the top corner (blue point in figure 7). Otherwise, it can be located on the border of two regions or in the red area. For the red area, all the points will converge to the stable equilibrium at the bottom corner (red equilibrium in figure 7), and if the initial network state locates exactly on the border (black line in figure 7), the system will converge to the unstable equilibrium. This situation is nearly impossible in practice.

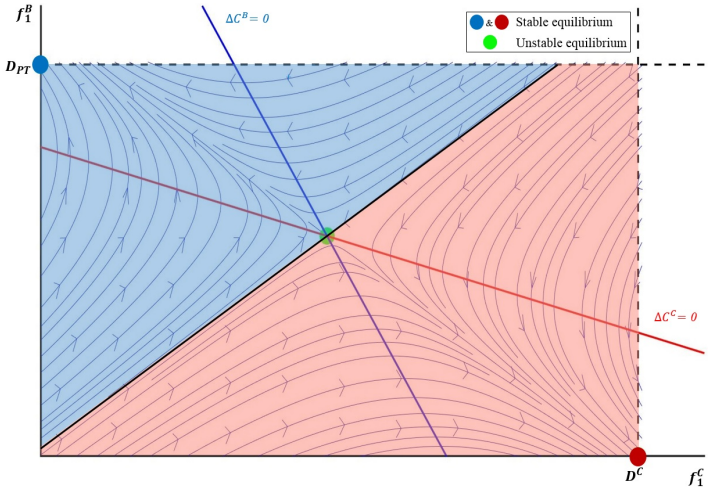

Figure 7. Cost-flow diagram based on path 1: The domain of convergence for each equilibrium

4. Non unicity of equilibrium states in multimodal STA

4.1. *Equilibrium analysis for Scenario 1: (car-bus)-train case*

In Scenario 1, We have $D^T = 0$ at the initial equilibrium state when only car and bus lines are active. Thus $D_{PT} = D^B$. Here, we want to investigate the situation where we have multiple equilibria, so let us assume that we have multiple solutions at the equilibrium state by holding conditions 22 and the cost of train is not always less than bus, i.e., $c_3^T \not< c_a^B; \forall f_a^m$. Figure 8 presents the nine possibilities for multiple equilibria according to the slope of two figures. These possibilities will be the starting point for

scenario 1, when the train line is added, and the convergence process starts. In figure 8, the unstable equilibrium is the intersection of two lines and presented by a point (I) and the two stable equilibria are points (P) and (Q).

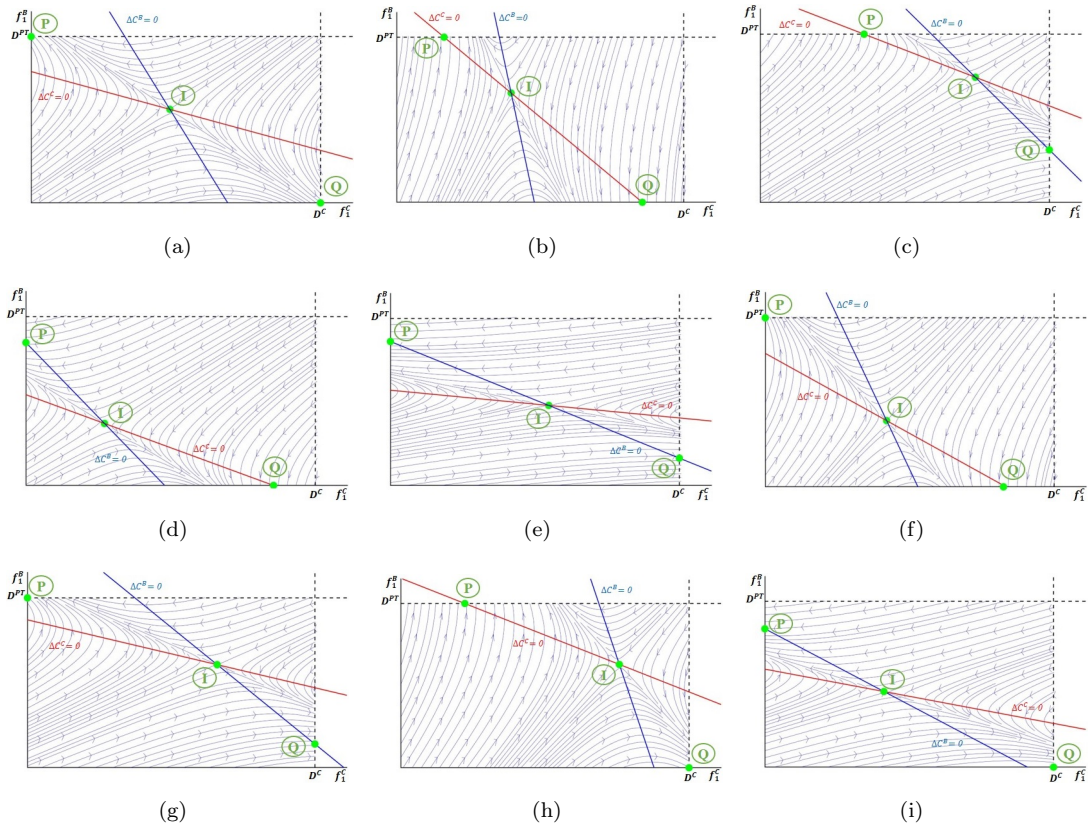

Figure 8. The equilibrium for the intermediate state of Scenario 1: The flow diagram of path 1 when $\rho_B > \rho_C$.

Before adding the train line, we need to analyze the variables and parameters for all cases in figure 8. Here, we consider figure 8(a) as an example for analysis and then presents the results for other test cases in figure 8.

4.1.1. car-bus equilibria in case of figure 8(a)

Before adding the train to the system, we need to analyze the two stable equilibria. For point (P), we have the following conditions:

$$\begin{cases} D^T = 0 \\ f_1^C = 0 \\ f_2^C = D^C \\ f_1^B = D_{PT} \\ f_2^B = 0 \end{cases} \tag{25}$$

Therefore, the OD cost and equilibrium constraints at point $\textcircled{P}$ are as follows:

$$\begin{cases} S^C(P) = c_2^C = g_2^C + h_2^{C,C} D^C \leq g_1^C + h_1^{C,B} D_{PT} \\ S^B(P) = c_1^B = g_1^B + h_1^{B,B} D_{PT} \leq g_2^B + h_2^{B,C} D^C \end{cases} \tag{26}$$

where, $S^m(x)$ is the OD cost for mode m at point x. Consequently, the feasibility conditions for the parameters are:

$$\begin{cases} g_1^C - g_2^C \geq h_2^{C,C} D^C - h_1^{C,B} D_{PT} \\ g_1^B - g_2^B \leq h_2^{B,C} D^C - h_1^{B,B} D_{PT} \end{cases} \tag{27}$$

In the same manner, we will have the following equations for point $\textcircled{Q}$:

$$\begin{cases} D^T = 0 \\ f_1^C = D^C \\ f_2^C = 0 \\ f_1^B = 0 \\ f_2^B = D_{PT} \end{cases} \tag{28}$$

$$\begin{cases} S^C(Q) = c_1^C = g_1^C + h_1^{C,C} D^C \leq g_2^C + h_2^{C,B} D_{PT} \\ S^B(Q) = c_2^B = g_2^B + h_2^{B,B} D_{PT} \leq g_1^B + h_1^{B,C} D^C \end{cases} \tag{29}$$

$$\begin{cases} g_1^C - g_2^C \leq h_2^{C,B} D_{PT} - h_1^{C,C} D^C \\ g_1^B - g_2^B \geq h_2^{B,B} D_{PT} - h_1^{B,C} D^C \end{cases} \tag{30}$$

Note that equations 27 and 30 are equivalent to the fact that (i) the intersects of $\Delta c^C = 0$ with $f_1^B = 0$ are not less than D^c; (ii) the intersects of $\Delta c^B = 0$ with $f_1^C = 0$ are not less than D^B. In addition, at the stable equilibrium state in this case, both paths are not used by one mode. Consequently, by considering $H^{m,\mu} = h_1^{m,\mu} + h_2^{m,\mu}$, we can summarize the compatibility conditions for set of parameters from the right side of equations 27 and 30:

$$\begin{cases} H^{C,C} D^C < H^{C,B} D_{PT} \\ H^{B,B} D_{PT} < H^{B,C} D^C \end{cases} \tag{31}$$

From equations 27 and 30, we deduce a conditions for the data parameters (D^C and $D_{PT} = D^B$) to yield the situation of figure 8(a). For instance, if $g_1^m = g_2^m$, then D^C and D_{PT} should satisfy the following condition:

$$max \left\{ \frac{h_1^{B,B}}{h_2^{B,C}}, \frac{h_2^{B,B}}{h_1^{B,C}} \right\} \leq \frac{D^C}{D_{PT}} \leq min \left\{ \frac{h_2^{C,B}}{h_1^{C,C}}, \frac{h_1^{C,B}}{h_2^{C,C}} \right\} \tag{32}$$

The equations 26, 29 and 31 provide the conditions for the parameters to generate a figure 8(a) type of situation. In the same way, we can calculate the parameter domains and equilibria set for other cases in figure 8. Table 2 presents the parameter domains for all cases in figure 8. The constraints in the table are necessary conditions for each case. The first two columns are the relations between the fixed cost of each mode on each link (g_a^m), the demand and the mode impact factors ($h_a^{m,\mu}$), i.e., similar to equations 26 and 29 for figure 8(a). The third column presents the summarized condition (similar to equation 31) for all cases. Recall that equation 22 guarantee the non-uniqueness while the conditions in table 2 distinguish different settings wherein we have multiple equilibria. The multiple equilibria is guaranteed for the intermediate state. Now, we can add train and discuss how the equilibrium change based on the cost of the train.

4.1.2. Adding train to the system

As shown in figure 4, we consider the three equilibria ($\textcircled{P}$, $\textcircled{Q}$, and $\textcircled{I}$) as the possible intermediate states, i.e., the starting point for the final convergence process of scenario 1. Now, we add the train to the system. If $c_3^T > g_a^B; \forall a \in A$, then the train is not used and does not change the system, also, if $c_3^T \leq g_a^B; \forall a \in A$, then the users stop using the bus and we will have two independent modes (car and train). The system converges to a unique equilibrium. The challenge is when the cost of the train is comparable to the cost of the bus, and the system moves to new equilibria. In the final state of the network, all modes are active. Therefore, according to equation 2:

$$D_{PT} = D^B + D^T \tag{33}$$

where D^B depends on D^T, which is determined by solving $c_3^T = c^B$.

For Δc^B, if the flow of bus shifts to the train line or the reverse, according to equations 11 and 33, lines $f_1^B = D^B$ and $\Delta c^B = 0$ are moved. Therefore, if $\Delta c^B > 0$ there is a possibility that a part of f_2^B is swapped with the train line and the network state point on the flow diagram does not move. Otherwise, as with the car, f_1^B increases and the network state moves up. Finally, when $\Delta c^B < 0$, f_1^B decreases and the solution moves down.

Indeed, when the train enters the system, two lines move in all cases in figure 8:

- Line $f_1^B = D_{PT}$: It changes to $f_1^B = D^B = D_{PT} - D^T$ and starts decreasing. If one user swaps from this pattern to the train, then the border is shifted down by 1 unit.
- Line $\Delta C_1^B = 0$: It moves to left and downwards because the flow of the bus shifts to the train. The rate of translation of this line if one user swaps to the train is $\frac{h^{m,B}}{H^{m,B}}$ according to the conditions 22.

Note that line $\Delta C_1^C = 0$ can move in some cases but the line translation directly depends on the translation of $\Delta C_1^B = 0$. The translation size of line $\Delta C_1^B = 0$ is smaller than line $f_1^B = D_{PT}$ ($\frac{h^{m,B}}{H^{m,B}} \leq 1$). Therefore, the line $f_1^B = D_{PT}$ can pass $\Delta C_1^B = 0$ or $\Delta C_1^C = 0$ and point $\textcircled{I}$ in all cases except figures 8(b), 8(c) and 8(h). The analysis of the final equilibrium based on the intermediate state is as follows:

(1) The intermediate state is point $\textcircled{I}$: According to the movement of the line, $m = B$ to the left and downwards, the system will converge to point $\textcircled{Q}$ in all cases in conditions 22.

Table 2. The parameter domains for different cases wherein we have multiple equilibria (figure 8).

Figure	Parameters conditions		
	$g_1^C - g_2^C$	$g_1^B - g_2^B$	Summarized conditions
8(a)	$\begin{cases} \leq h_2^{C,B} D_{PT} - h_1^{C,C} D^C \\ \geq h_2^{C,C} D^C - h_1^{C,B} D_{PT} \end{cases}$	$\begin{cases} \leq h_2^{B,C} D^C - h_1^{B,B} D_{PT} \\ \geq h_2^{B,B} D_{PT} - h_1^{B,C} D^C \end{cases}$	$\begin{cases} H^{C,C} D^C < H^{C,B} D_{PT} \\ H^{B,B} D_{PT} < H^{B,C} D^C \end{cases}$
8(b)	$\begin{cases} < h_2^{C,C} D^C - h_1^{C,B} D_{PT} \\ > h_2^{C,B} D_{PT} - h_1^{C,C} D^C \end{cases}$	$\begin{cases} \leq h_2^{B,C} D^C - h_1^{B,B} D_{PT} - \frac{H^{B,C}}{H^{C,C}} (g_2^C - g_1^C + h_2^{C,C} D^C - h_1^{C,B} D_{PT}) \\ \geq h_2^{B,B} D_{PT} + h_2^{B,C} D^C - \frac{H^{B,C}}{H^{C,C}} (g_2^C - g_1^C + h_2^{C,C} D^C + h_2^{C,B} D_{PT}) \end{cases}$	$\begin{cases} H^{C,C} D^C > H^{C,B} D_{PT} \\ H^{B,B} H^{C,C} < H^{B,C} H^{C,B} \end{cases}$
8(c)	$\begin{cases} < h_2^{C,C} D^C - h_1^{C,B} D_{PT} \\ \leq h_2^{C,B} D_{PT} - h_1^{C,C} D^C - \frac{H^{C,B}}{H^{B,B}} (g_2^B - g_1^B + h_2^{B,B} D_{PT} - h_1^{B,C} D^C) \end{cases}$	$\begin{cases} < h_2^{B,B} D_{PT} - h_1^{B,C} D^C \\ \leq h_2^{B,C} D^C - h_1^{B,B} D_{PT} - \frac{H^{B,C}}{H^{C,C}} (g_2^C - g_1^C + h_2^{C,C} D^C - h_1^{C,B} D_{PT}) \end{cases}$	$\begin{cases} H^{C,C} D^C > g_2^C - g_1^C + h_2^{C,C} D^C - h_1^{C,B} D_{PT} \\ H^{B,B} D_{PT} > g_2^B - g_1^B + h_2^{B,B} D_{PT} - h_1^{B,C} D^C \end{cases}$
8(d)	$\begin{cases} > h_2^{C,B} D_{PT} - h_2^{C,C} D^C \\ \geq h_2^{C,B} D_{PT} + h_2^{C,C} D^C - \frac{H^{C,B}}{H^{B,B}} (g_2^B - g_1^B + h_2^{B,B} D_{PT} + h_2^{B,C} D^C) \end{cases}$	$\begin{cases} > h_2^{B,C} D^C - h_2^{B,B} D_{PT} \\ \geq h_2^{B,C} D^C + h_2^{B,B} D_{PT} - \frac{H^{B,C}}{H^{C,C}} (g_2^C - g_1^C + h_2^{C,C} D^C + h_2^{C,B} D_{PT}) \end{cases}$	$\begin{cases} g_1^C - g_2^C < h_2^{C,C} D^C + h_2^{C,B} D_{PT} \\ g_1^B - g_2^B < h_2^{B,B} D_{PT} + h_2^{B,C} D^C \end{cases}$
8(e)	$\begin{cases} \leq h_2^{C,B} D_{PT} - h_1^{C,C} D^C - \frac{H^{C,B}}{H^{B,B}} (g_2^B - g_1^B + h_2^{B,B} D_{PT} - h_1^{B,C} D^C) \\ \geq h_2^{C,B} D_{PT} + h_2^{C,C} D^C - \frac{H^{C,B}}{H^{B,B}} (g_2^B - g_1^B + h_2^{B,B} D_{PT} + h_2^{B,C} D^C) \end{cases}$	$\begin{cases} < h_2^{B,B} D_{PT} - h_1^{B,C} D^C \\ > h_2^{B,C} D^C - h_1^{B,B} D_{PT} \end{cases}$	$\begin{cases} H^{B,C} D^C < H^{B,B} D_{PT} \\ H^{B,B} H^{C,C} < H^{B,C} H^{C,B} \end{cases}$
8(f)	$\begin{cases} < h_2^{C,C} D^C + h_2^{C,B} D_{PT} \\ \geq h_2^{C,C} D^C - h_1^{C,B} D_{PT} \end{cases}$	$\begin{cases} \leq h_2^{B,C} D^C - h_1^{B,B} D_{PT} \\ \geq h_2^{B,B} D_{PT} + h_2^{B,C} D^C - \frac{H^{B,C}}{H^{C,C}} (g_2^C - g_1^C + h_2^{C,C} D^C + h_2^{C,B} D_{PT}) \end{cases}$	$\begin{cases} g_1^C - g_2^C > h_2^{C,B} D_{PT} - h_1^{C,C} D^C \\ H^{B,B} H^{C,C} D_{PT} < H^{B,C} (g_2^C - g_1^C + h_2^{C,C} D^C + h_2^{C,B} D_{PT}) \end{cases}$
8(g)	$\begin{cases} \leq h_2^{C,B} D_{PT} - h_1^{C,C} D^C - \frac{H^{C,B}}{H^{B,B}} (g_2^B - g_1^B + h_2^{B,B} D_{PT} - h_1^{B,C} D^C) \\ \geq h_2^{C,C} D^C - h_1^{C,B} D_{PT} \end{cases}$	$\begin{cases} \leq h_2^{B,C} D^C - h_1^{B,B} D_{PT} \\ > -h_1^{B,B} D_{PT} - h_1^{B,C} D^C \end{cases}$	$\begin{cases} H^{B,B} H^{C,C} D^C < H^{C,B} (g_1^B - g_2^B + h_1^{B,C} D^C + h_1^{B,B} D_{PT}) \\ g_1^B - g_2^B < h_2^{B,B} D_{PT} - h_1^{B,C} D^C \end{cases}$
8(h)	$\begin{cases} \leq h_2^{C,B} D_{PT} - h_1^{C,C} D^C \\ > -h_1^{C,B} D_{PT} - h_1^{C,C} D^C \end{cases}$	$\begin{cases} \leq h_2^{B,C} D^C - h_1^{B,B} D_{PT} - \frac{H^{B,C}}{H^{C,C}} (g_2^C - g_1^C + h_2^{C,C} D^C - h_1^{C,B} D_{PT}) \\ \geq h_2^{B,B} D_{PT} - h_1^{B,C} D^C \end{cases}$	$\begin{cases} g_1^C - g_2^C < h_2^{C,C} D^C - h_1^{C,B} D_{PT} \\ H^{B,B} H^{C,C} D_{PT} < H^{B,C} (g_1^C - g_2^C + h_1^{C,B} D_{PT} + h_1^{C,C} D^C) \end{cases}$
8(i)	$\begin{cases} \leq h_2^{C,B} D_{PT} - h_1^{C,C} D^C \\ \geq h_2^{C,B} D_{PT} + h_2^{C,C} D^C - \frac{H^{C,B}}{H^{B,B}} (g_2^B - g_1^B + h_2^{B,B} D_{PT} + h_2^{B,C} D^C) \end{cases}$	$\begin{cases} < h_2^{B,C} D^C + h_2^{B,B} D_{PT} \\ \geq h_2^{B,B} D_{PT} - h_1^{B,C} D^C \end{cases}$	$\begin{cases} H^{B,B} H^{C,C} D^C < H^{C,B} (g_2^B - g_1^B + h_2^{B,C} D^C + h_2^{B,B} D_{PT}) \\ g_1^B - g_2^B > h_2^{B,C} D^C - h_1^{B,B} D_{PT} \end{cases}$

(2) The intermediate state is point $\textcircled{Q}$: Any movement of the equilibrium will place the starting point (intermediate state) in the region where the PDS$(f, \Delta c(f))$ pushes the system to the updated point $\textcircled{Q}$. Thus, the system converges to the unique equilibrium.
(3) The intermediate state is point $\textcircled{P}$: As with the previous case, any movement of the equilibrium places the intermediate state in the region that converges to the updated point $\textcircled{P}$.

We can calculate the new equilibrium $\bar{P}$ or $\bar{Q}$ by considering the initial equilibrium. For instance, at $\textcircled{\bar{P}}$ if the initial state is P, then we have:

$$S^B(\bar{P}) = g_1^B + h_1^{B,B}(D_{PT} - D^T) = C_3^T = S^B(P) - \epsilon = S^B(P) - h_1^{B,B} D^T \tag{34}$$

where ϵ is the difference between C_3^T and the cost of bus at P. Therefore, $D^T = \frac{\epsilon}{h_1^{B,B}}$ and based on equation 33, we have:

$$D^B(\epsilon) = D_{PT} - \frac{\epsilon}{h_1^{B,B}} \tag{35}$$

To complete this example, if equation 32 is satisfied, we obtain a stable equilibrium at point $\textcircled{\bar{P}}$:

$$\begin{cases} f_1^C = 0 \\ f_2^C = D^C \\ f_1^B = D^B(\epsilon) \\ f_2^B = 0 \end{cases} \tag{36}$$

In the same way, we can calculate the updated equilibria Q and I.

In order to represent the trajectory of the intermediate solutions toward the final equilibrium, we need to extend the projected dynamical system. It should be remembered that we consider the train as an independent travel mode, which has an impact on the demand for the bus. In this case, the flow vector of independent flows $(\dot{f})$, the feasible domain K for the independent flow variables, and the field variables (Δc) are as follows:

$$f = (f_1^C, f_1^B, D^T) \tag{37}$$

$$\begin{cases} 0 \leq f_1^C \leq D^C \\ 0 \leq f_1^B + D^T \leq D_{PT} \end{cases} \tag{38}$$

$$\Delta c = \begin{cases} \Delta c^C = c_2^C - c_1^C \\ \Delta c^B = c_2^B - c_1^B \\ \Delta c^T = \min\{c_1^B, c_2^B\} - c_3^T \end{cases} \tag{39}$$

Therefore, $K = [0, D^C] \times [0, D_{PT}] \times [0, D_{PT}]$ is shown in figure 9.

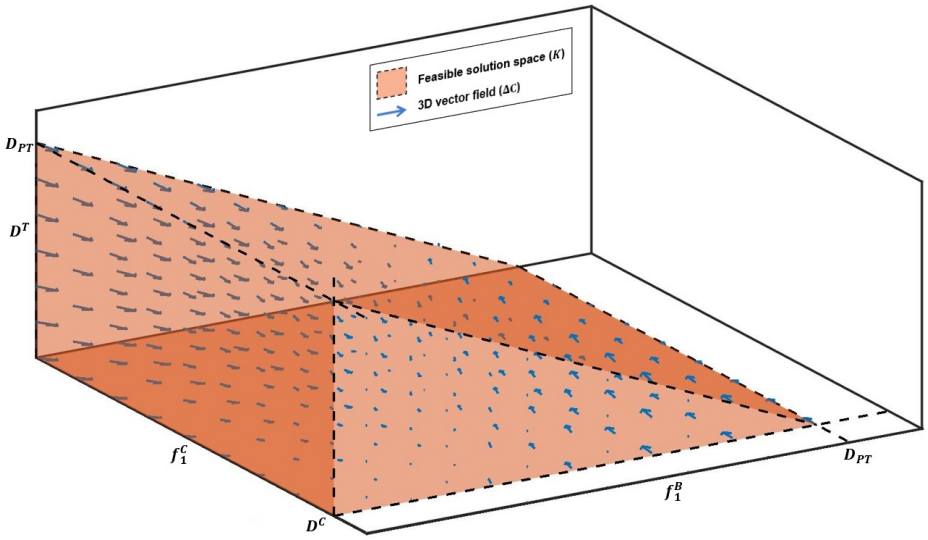

Figure 9. The feasible solution space (K) when all modes are active

The PDS($f, \Delta c(f)$) is defined by equation 16 with f is given by equation 37 and $\Delta c(f)$ is given by equation 39. Same as the previous section, the network equilibria are the fixed points of PDS($f, \Delta c(f)$) in K. At each point in K we have a 3D field vector (figure 9) that moves the solution toward the final equilibrium. Figure 10 presents an example for Scenario 1, wherein the cost of the train is comparable with bus lines. The three possible starting points corresponding to the intermediate network state (final equilibria for car-bus network) are presented with red squares, and green field lines represent the trajectory of solution from the intermediate solution (car-bus equilibrium) toward the final equilibrium when all modes are active.

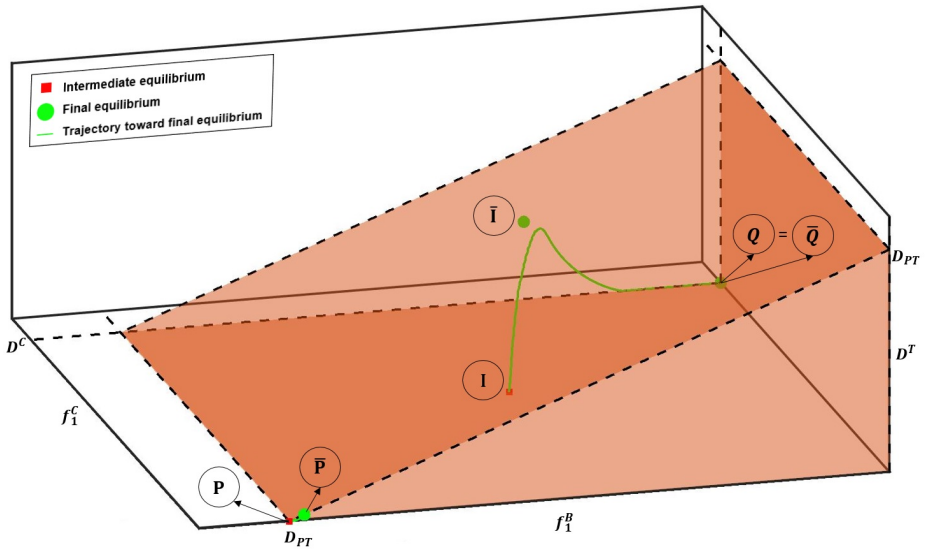

Figure 10. The trajectory of the intermediate solution in Scenario 1 toward the final equilibrium.

Consequently, for the first scenario, we could have two different stable equilibria by adding a new mode even if the infrastructure is independent. It should be noted that the

final equilibrium state of Scenario 1 depends on the initial state which is determined by bi-modal equilibrium (section 3), i.e., the network design history defines which states can be the final ones.

4.2. *Equilibrium analysis for Scenario 2: (car-train)-bus case*

4.2.1. Car-train equilibrium analysis

For the second scenario, the intermediate state is the equilibrium state of the system when just car and train are active ($f_m^B = 0\ ; \forall m$). Therefore, We have two independent modes with fixed demand. In this case, the equilibrium is unique because $D^T = D_{PT}$, i.e., the totality of public transportation demand is assigned to train, and there are two independent linear strictly monotone functions for cars.

$$\begin{cases} c_1^C = g_1^C + h_1^{C,C} f_1^C \\ c_2^C = g_2^C + h_2^{C,C} f_2^C \end{cases} \tag{40}$$

The demand D^C is split between paths 1 and 2. Finally, we have one of the following possibilities as a function of $g_a^C, h_a^{C,C}\ ; \forall a$:

- Only path 1 is used: $f_1^C = D^C \quad ; \quad f_2^C = 0 \quad ; \quad C_1^C \leq C_2^C$
- Only path 2 is used: $f_1^C = 0 \quad ; \quad f_2^C = D^C \quad ; \quad C_1^C \geq C_2^C$
- Both path are used: $f_1^C, f_2^C \geq 0 \quad | \quad C_1^C = C_2^C \quad ; \quad f_1^C + f_2^C = D^C$

The domain for a unique starting point for scenario 2: (x^*, y^*, z^*) is $\{x^* \in [0, D^C], y^* = 0, z^* = D_{PT}\}$ where is located in the flow diagram of path 1 and path 3 (figure 9) at the intersect of $\Delta c^C = 0$ with $f_1^B = 0$. The unique equilibrium for car and train network on the path flow diagram of path 1 is as follows:

$$\begin{cases} D^T = D_{PT} \\ f_1^C = \frac{g_2^C - g_1^C + h_2^{C,C} D^C}{H^{C,C}} \\ f_1^B = 0 \end{cases} \tag{41}$$

4.2.2. Adding bus to the system

When the bus lines are added to the system, the initial situation is the car-train equilibrium and the cost for bus lines are:

$$\begin{cases} c_1^B = g_1^B + h_1^{B,C} f_1^C \\ c_2^B = g_2^B + h_2^{B,C} (D^C - f_1^C) \end{cases} \tag{42}$$

where f_1^C is given by equation 41. The minimum OD cost for bus at the car-train equilibrium point is:

$$S^B(\mathrm{C} + \mathrm{T}) = min\left\{c_1^B, c_2^B\right\} \tag{43}$$

If the $c_3^T \leq S^B(\mathrm{C} + \mathrm{T})$, public transportation travellers have no incentive to switch mode to bus. From a mathematical point of view, Δc^m remains at zero and the

PDS($f, \Delta c(f)$) cannot move the point. Otherwise ($c_3^T > S^B(\mathrm{C} + \mathrm{T})$), if only path 1 or both paths are used, the convergence process starts in the region where the intermediate solution is located pushes the system to point $\bar{Q}$. If only path 2 is used ($f_1^C = 0$), the final equilibrium depends on the mode cost functions. In this case, one of two stable equilibria (points $\bar{P}$ and $\bar{Q}$) can be reached.

Figure 11 presents two configurations of Scenario 2 wherein the intermediate equilibrium converges to two different equilibria. For each configuration the trajectory towards the equilibrium (PSD field-line) is depicted.

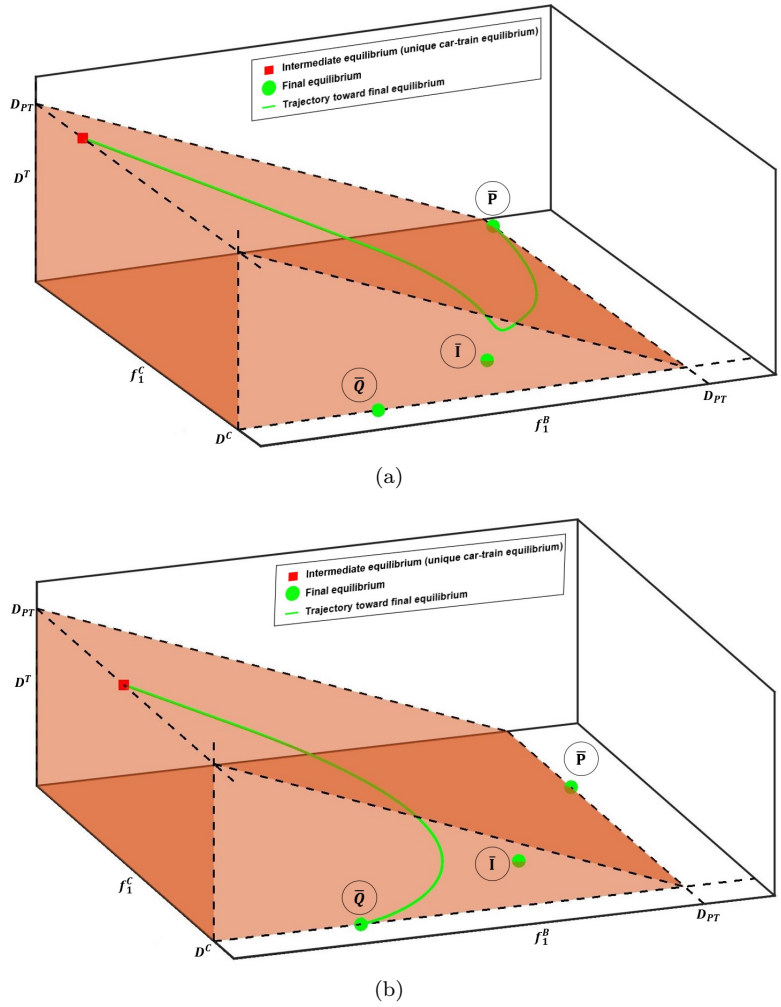

Figure 11. The intermediate solution trajectory in Scenario 2 toward the final equilibrium when $c_3^T > S^B(\mathrm{C} + \mathrm{T})$.

In figure 11(a), the configuration of the (car-bus) problem is same as figure 8(c) and $c_3^T > S^B(\mathrm{C} + \mathrm{T})$. The three final equilibria are located on the plain of (f_1^C, f_1^B) and the intermediate solution (car-train equilibrium by equation 41) leads us to $\bar{Q}$. By increasing $h_2^{C,C}$ with respect to the corresponding constraints in table 2, the configuration of figure 11(b) is obtained, where the final equilibrium is $\bar{P}$ based on the intermediate solution (equation 41). We can conclude that if multiple equilibria are possible for the final state, the initial car-train equilibrium determines which equilibrium will be reached at the end of the second scenario.

4.3. *Equilibrium analysis for Scenario 3: car-bus-train case*

In the third scenario, we have only one phase wherein all modes are active. The initial state of the network can be any path flow distribution in K (figure 9). The initial condition to have multiple equilibria is $c_3^T \not< g_a^B; \forall a \in A$, which means that the cost of the train is not always less than the cost of the bus lines. Otherwise, only cars and trains will be used, where both modes are independent, and consequently the equilibrium is unique. Moreover, if we have $c_a^B \not< c_3^T; \forall f_a^m$, which means that C_3^T is comparable with the cost of the bus, so at the equilibrium state a part of D_{PT} takes the train (like equilibrium $\widehat{(P)}$ in figure 10). Otherwise, the train will not be used ($D^T = 0$), and we could have multiple equilibria based on the analysis in section 3. Consequently, for scenario 3, we will have conditional equilibrium based on the values ρ_C, ρ_B, and c_3^T.

$$\text{Solution set} = \begin{cases} c_3^T < c_a^B; \forall a, f_a^m \rightarrow 1 \text{ equilibrium with } D^T = D_{PT}, \\ o.w. \rightarrow \begin{cases} \rho_B > \rho_C \rightarrow \begin{cases} (\Delta c^C = 0) \cap (\Delta c^B = 0) \in K \rightarrow 3 \text{ equilibria}, \\ o.w. \rightarrow 1 \text{ equilibrium}, \end{cases} \\ \rho_B < \rho_C \rightarrow 1 \text{ equilibrium}. \end{cases} \end{cases} \tag{44}$$

In the case of multiple equilibria, based on the initial path flow distribution, we can converge to three possible equilibria based on the day-to-day process. Consequently, similar to bi-modal equilibria, the initial state of the network, determines the final equilibrium in Scenario 1.

To conclude this section, figure 12 presents the relation between the intermediate state of the network and the final equilibrium with a different order of mode activation. In order to clarify the findings of this section, figure 13 presents an example wherein with different network design history, the system converges to different equilibrium. The configuration of this example is based on figure 8(e) and corresponding condition in table 2. Figures 13(a) and 13(b) present Scenario 1. We choose the uniform flow propagation for the initial solution. The intermediate equilibrium in the car-bus network is obtained based on the projected dynamical system (figure 13(a)). Then we add the train line to the system and calculate the final equilibrium (figure 13(b)). Figure 13(c) presents Scenario 2, wherein the intermediate equilibrium is the unique one from the car-train network. The results show that with a different order of mode activation, the system reaches to different equilibrium.

This study shows that even in the linear STA, if we have a different order for opening the new network facility (table 1) and even with a rational learning process, we converge to different equilibrium. In other words, we showed that even in a small and simple network, when the multiple equilibria are guaranteed (equation 22 and table 2), the network design history has a significant impact on the final equilibrium that is reached by the system. Note that the equilibration of the first step to find the intermediate equilibrium is not necessarily finished in practice before the second step starts. It depends on the frequency of new options integration versus the time requires for a stable equilibrium to be achieved.

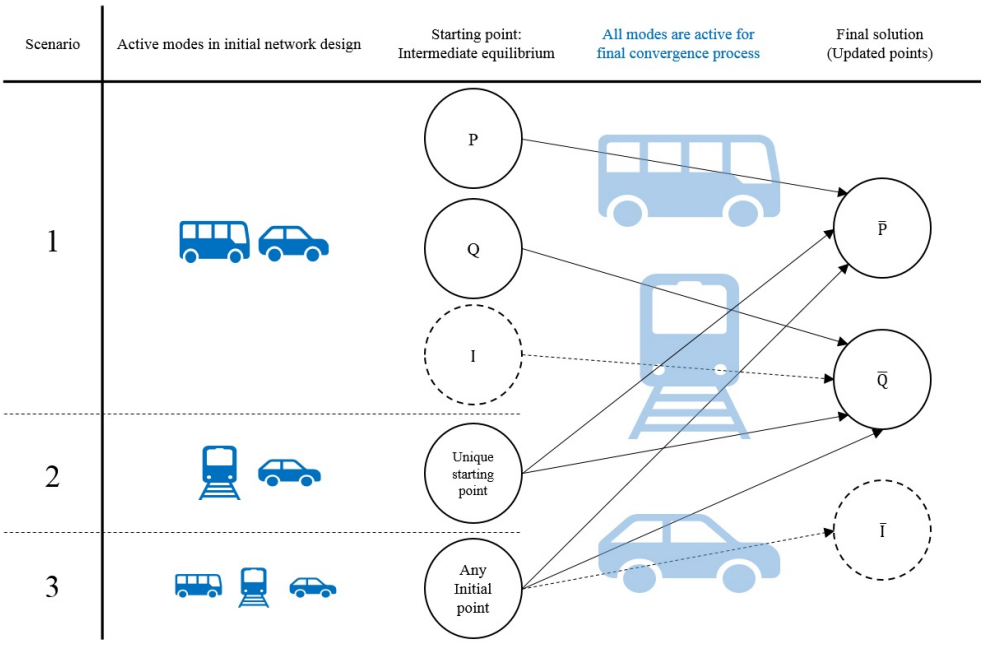

Figure 12. The convergence of scenarios for the mono-OD test case. [Dash lines presents rare situations wherein the initial point is located at unstable equilibrium]

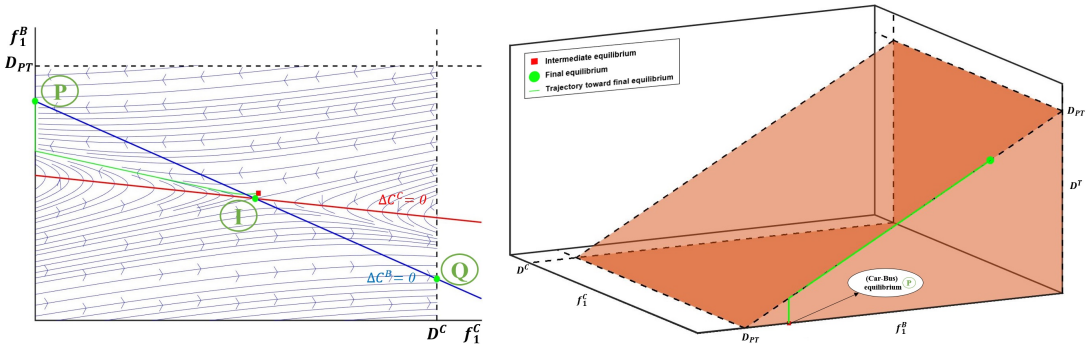

(a) Car-Bus equilibrium convergence with initial solution: $f_1^m = (\frac{D^C}{2}, \frac{D_{PT}}{2})$.

(b) (Car-Bus)-Train equilibrium convergence. The intermediate equilibrium comes from Figure 13(a)

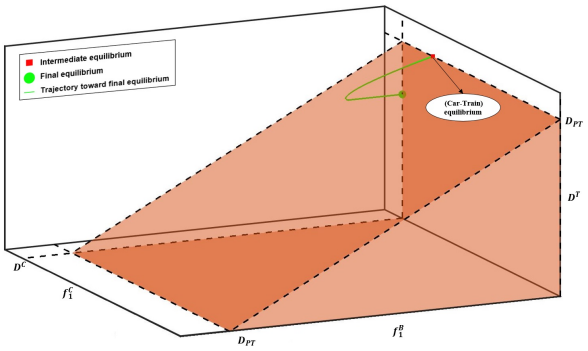

(c) (Car-Train)-Bus equilibrium convergence.The intermediate equilibrium comes from equation 41.

Figure 13. The impact of network design history on the final equilibrium of figure 8(e).

5. Multi-modal simulation-based day-to-day DTA

In this section, we address the question of network history and multiple multimodal user equilibria in a more realistic framework. Now, we resort to a dynamic traffic simulator for the network loading and focus on a real network. Although the setting is more complex, mechanisms similar to those described in the previous section apply and induce non unicity of equilibria, and dependence of equilibria to the order of activation of facilities.

5.1. *Day-to-day network equilibrium model*

Consider a network $G(N, A)$ with a finite set of nodes N and a finite set of directed links A. The period of interest (planning horizon) of duration D is D_{max} days indexed by d ($d \in D = \{0, 1, 2, ..., D_{max}\}$). In a day d, travel time and traffic conditions are calculated by simulation and the users choose the path for the next day based on the travel time experienced during the current day. The important notations for introducing the dynamic equilibrium model are as follows:

W: set of OD pairs.
P_w^d: set of paths for w in day d.
w: index of OD pair, $w \in W$.
p: index of path, $p \in P_{w,d}$.
$\pi_{w,p}^d$: number of users from an OD pair w that are assigned to path p in day d.
C_p^d: Cost of path p in day d.
C_w^{d*}: minimum Cost of OD pair w in day d.

Note that P_w^d is not necessarily equal to P_w^{d+1} because the network design can be changed, i.e., the new transportation facility is added to the network from the next day $(d+1)$.

In the trip-based DTA problem, we consider each user as a particle in the network. Thus, the solution space is discrete and the goal according to UE discipline is to minimize the gap between path travel time and the shortest path travel time of the related OD pair for all OD pairs (Djavadian and Chow 2017), which is equivalent to equation 5. In other words, finding the UE situation is equivalent to minimizing the delay of each user compared to the optimal option of the associated OD pair (shortest path) in the network. Using this definition, for each OD pair $w \in W$ and for all paths $p \in P_{w,d}$, the dynamic traffic network equilibrium with a given travel demand and user departure time for the trip-based DTA model is reached on day $d \in D$ if the following conditions are satisfied (Wardrop 1952):

$$\begin{cases} C_p^d - C_w^{d*} \geq 0 \\ \pi_{w,p}^d (C_p^d - C_w^{d*}) = 0 \\ \pi_{w,p}^d \geq 0 \end{cases} \tag{45}$$

Based on equation 45, we can define a quality indicator for the solutions which is calculated as the average delay of the network (Janson 1991) for day d:

$$AG^d = \frac{\sum_{w \in W} \sum_{p \in P_w^d} (C_p^d - C_w^{d*})}{\sum_{w \in W} \sum_{p \in P(w,d)} \pi_{w,p}^d} \tag{46}$$

Note that $AG^d = 0$ when the perfect UE path flow distribution is achieved. The aim of the day-to-day process is to minimize the Average Gap of the network by considering the learning curve of the users.

At the end of each day, the users are ranked based on the TC they experience and 50% of users with the highest TC are allowed to swap to the time-dependent shortest path(s). The swap decision is taken by each user based on the Bernoulli trial:

$$P(S^d = 1) = \frac{EC - EC_w^*}{EC} \tag{47}$$

where S^d denotes the binary swap decision variable for day d, EC denotes the TC experienced by the user on the current day and EC_w^* denotes the minimum TC experienced of the OD pair w on the current day which is related to the user. Following the result of the trial, the user decides to swap or not. The day-to-day DTA framework is presented in figure 14, and detailed in the following:

(1) Read network and demand: The network and demand of the scenario designed are configured.
(2) Initialization: The initial paths are assigned to the users based on the scenario of the experiment.
(3) Traffic simulation: The simulation is executed for the inputs, and the simulator calculates all variables.
(4) All cost functions are calculated by the updated variables from the simulation.
(5) Identify the shortest path based on network facilities and access permission of users.
(6) Calculate the indicators and check the End condition based on Average Gap (equation 46):
    - **IF** Average Gap does not change, End the process
    - **ELSE** Update the path flow distribution for the next day by day-to-day process (equation 47).

5.2. *Dynamic simulator*

In this work, we use Symuvia, an open-source traffic simulator (https://github.com/Ifsttar/Open-SymuVia), as a trip-based simulator for calculating the travel costs in the network. Here, travel costs reduce to experienced travel times. Symuvia gives access to the position, speed, and acceleration of each vehicle (user) on the network. It is a microscopic simulator based on the Lagrangian resolution of the LWR (Lighthill Whitham Richards) model (Leclercq, Laval, and Chevallier 2007) which is the conservation law with respect to traffic density. Vehicle movements at the microscopic scale are governed by car-following principles with parameters related to vehicle categories (Leclercq 2007a,b), lane-changes by using a macroscopic

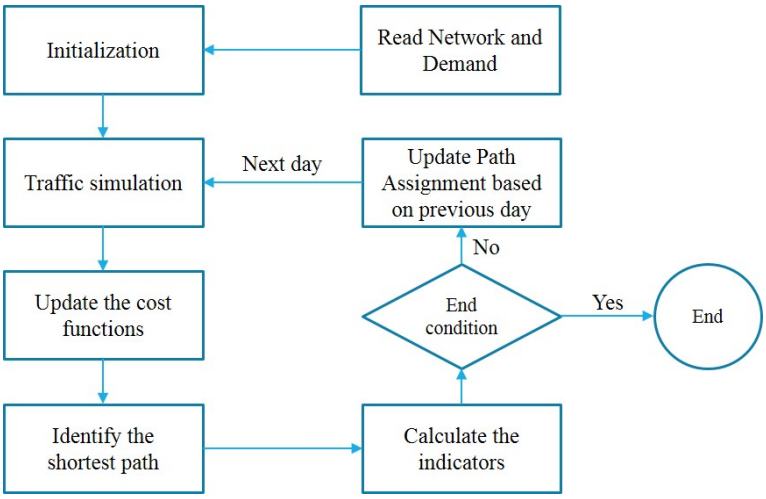

Figure 14. The day-to-day framework

theory of vehicle lane-changing inside microscopic models (Laval and Leclercq 2008), and shortest path calculation and assignment process by using column generation approach (Ameli, Lebacque, and Leclercq 2020). It has a simulation time-step equal to 1 second; travel time information is aggregated at the link level every 1 minute. The travel demand is given (dynamic OD pair demand), and users' routes are determined by a day-to-day DTA model, which guides each vehicle in the network on the route.

5.3. *Dynamic test case*

Using a dynamic simulator permits us to consider the large-scale network of Lyon 6e + Villeurbanne (figure 15(a)) with 1,883 Nodes, 3,383 Links, 94 Origins, 227 Destinations and 54,190 trips. Walking, buses and private cars are initially available transportation modes in the network. Figure 15(b) presents 31 bus lines in the Lyon 6e + Villeurbanne network includes 176 bus station (figure 15(c)). There are three metro lines (A, B and C) and 25 metro stations in the network (figure 15(d)). Each metro station has parking facilities. Carparks are the connectors between the metro grid and the traffic network. Therefore, the traveler can start their trip with a private car then use the carpark to take the metros. All mode changes during a trip introduce walking time for connection and possibly a waiting time for the next bus or metro to arrive at the station.

The network is loaded with travelers of all ODs with a given departure time in order to represent 1.5 hours of the network with the demand level based on the study of (Krug, Burianne, and Leclercq 2019). The goal is to analyze the final equilibrium solution obtained by a day-to-day DTA model with different settings corresponding to different successive introductions of the metro lines.

5.4. *Experiment scenarios*

For each scenario of opening metro lines, we run the day-to-day DTA for 300 days. A quarter of users only have access to the public transportation system (bus and metro) and the other three quarters have access to all transportation facilities (private car, bus, and metro) in the network. Note that bus lines are active for all scenarios. We can open three metro lines at the same time and calculate the equilibrium or successively

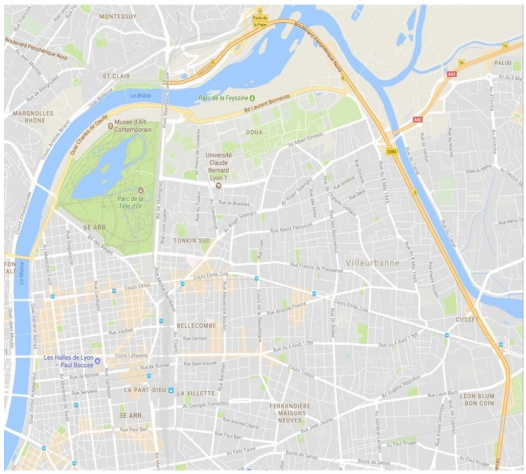

(a) Lyon 6e + Villeurbanne: Mapping data ©Google 2020.

(b) 31 bus lines.

(c) 176 bus station

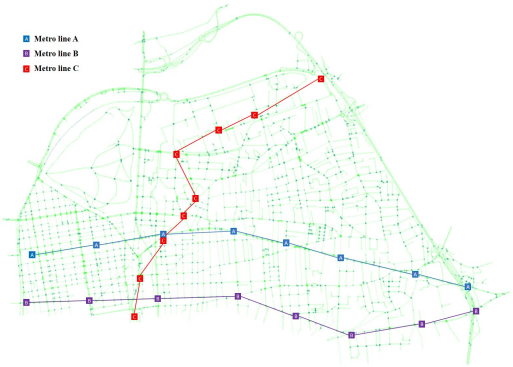

(d) 3 metro lines

Figure 15. Multimodal traffic network of Lyon 6e + Villeurbanne

open one metro line every 100 days and look for the final network state after 300 days. From the viewpoint of optimization, it means we change the intermediate assignment pattern to find the equilibrium. There are seven possible orders to activate the metro lines (figure 16). All the scenarios are started by the final equilibrium solution of the network without metro lines. The initial assignment pattern of each step is the final equilibrium flow distribution of the previous step (for more details see apendix A). For Scenario 1, all three metro lines are activated at the same time and once the day-to-day process is executed in order to equilibrate the system.

6. Numerical results

The full day-to-day process is conducted for all the scenarios, and we verify that all the simulations converge to a satisfactory UE solution, i.e., the Average Gap of all scenarios is less than 12 seconds, which shows good quality for the equilibrium in the large-scale network and given the demand level. Figure 17 (excluding 9h) presents the convergence pattern of the last step of all the scenarios. For instance, figure 17(b) presents the convergence pattern of the last step of the ABC scenario, which means

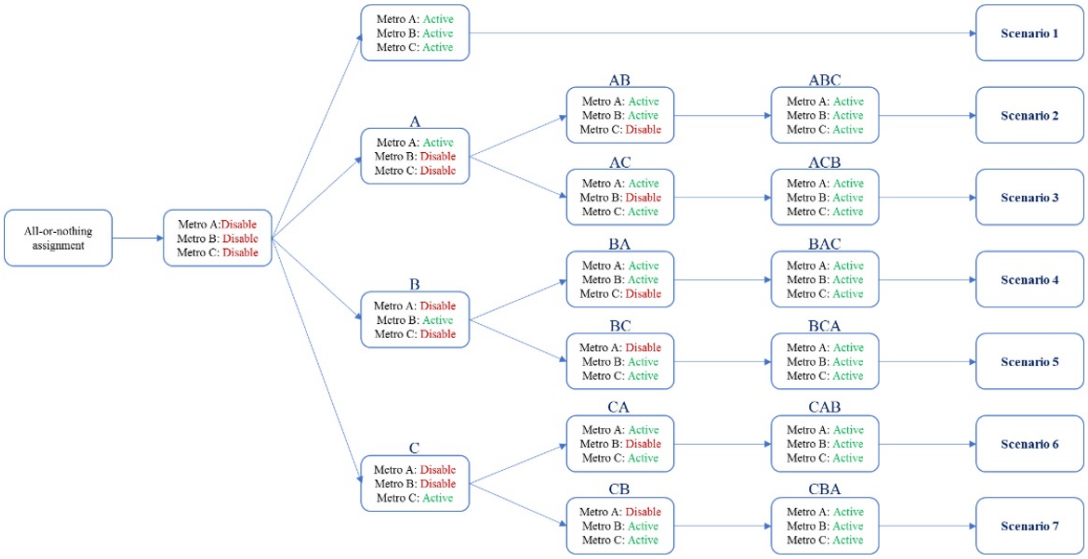

Figure 16. Chart of experiments

the simulation starts in the network with all the metro lines, with the equilibrium flow distribution of the AB simulation. The final solution of the AB simulation is obtained by the day-to-day process in the network wherein only metro lines, A and B, are active, and metro line C is deactivated (see figure 16). Mathematically speaking, all the convergence patterns correspond to the same final network design, including three metro lines with different intermediate steps.

Scenario 1 (A&B&C) starts with the equilibrium solution of the network without metro lines, and three metro lines become active at the same time for the last convergence process. This explains why the initial Average Gap of this scenario is much larger than others and the variation of the Average Gap is larger than in the other figures because the three new public transportation modes become active at the same time. It should be remembered that the day-to-day process stops when the Average Gap does not change for two consecutive days, which occurs for all the scenarios before day 46. Next, we evaluate the final solution in order to investigate the unicity of the solution.

We calculate the Violation indicator for the final path flow distribution of each scenario with the following steps:

(1) We assign a binary variable to each user in order to evaluate user violation (UV) by the following equation:

$$UV = \begin{cases} 1; & \text{if } \frac{EC_w - EC_w^*}{EC_w^*} \geq \epsilon \\ 0; & \text{o.w.} \end{cases} \tag{48}$$

(2) Compute the OD violation: the OD pair w is in violation when there are more than $\epsilon'; 0 \leq \epsilon' \leq 1$ of the users on w are in violation. The function ODV_w defines the OD violation.
(3) The network Violation indicator of network G is the share of ODs which are in violation.

Note that, similar to Average Gap, the perfect UE means network Violation equal to

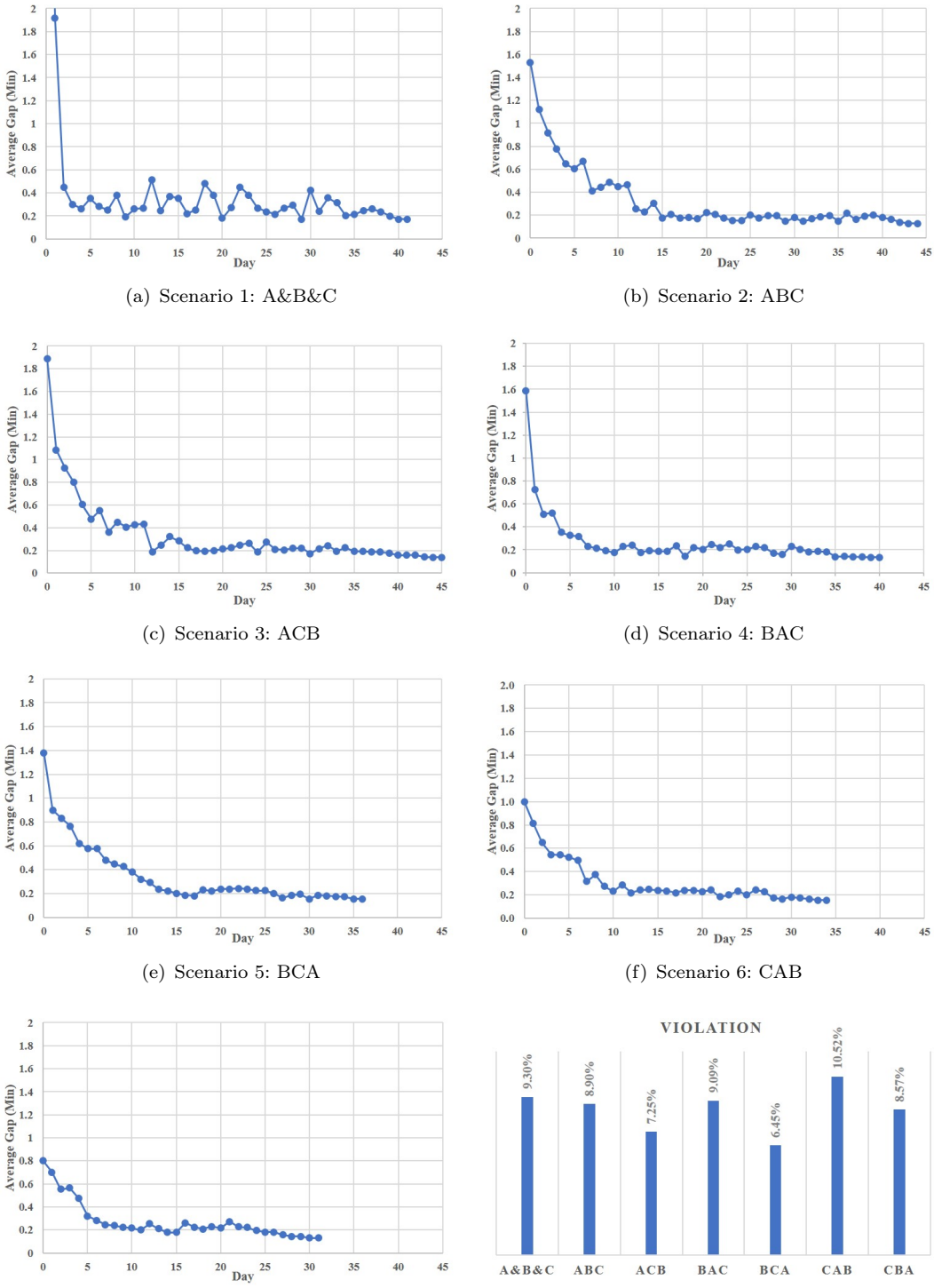

(a) Scenario 1: A&B&C

(b) Scenario 2: ABC

(c) Scenario 3: ACB

(d) Scenario 4: BAC

(e) Scenario 5: BCA

(f) Scenario 6: CAB

(g) Scenario 7: CBA

(h) Violation of final solution for all scenarios.

Figure 17. The average gap and violation in the day-to-day process for the final phase of all the scenarios.

zero with $\epsilon = \epsilon' = 0$ but in practice with trip-based simulation, it is more appropriate to set up a margin so that the values of ϵ and ϵ' are fixed at 10% in this study. Figure 17(h) presents the network Violation of the final solution of each scenario. The

results show that the quality of each solution is slightly different.

To evaluate the travel time distribution of OD pairs, we calculate the mean travel time and the percentage of failed trips for five most crowded OD pairs (highest demand level). A user fails the trip if they cannot arrive at their destination before the end of the simulation period. It is not a real failure as it usually simply means that users would arrive later after the end of the studied simulation period. The results are shown in table 3. The variation of Mean travel time and % trip failed shows that the path flow distribution of the scenario equilibria are different. For instance, the values of both indicators for scenario BAC are completely different from the other scenarios, and no two scenarios obtain similar equilibria.

Scenario CBA has minimum mean OD travel time for ODs 1 and 2 but the % trip failed is not minimum for OD 1. This explains that the impact of the other ODs path flow distributions prevent several users from finishing their trip even when the corresponding OD mean travel time is minimum. The system can choose a specific order for opening metro lines to minimize the mean OD travel time or % trip failed of targeted OD(s). For ODs 3 and 4, scenario CAB provides a minimum mean OD travel time and % trip failed, and finally scenario BCA has minimum indicators for OD 5.

Table 3. Mean travel time (Mean OD TT) [min] and percentage of failed trips (% trip failed) for top five most crowded OD pairs

Scenario \OD		1	2	3	4	5
A&B&C	% trip failed	5.1%	6.3%	2.0%	2.1%	6.5%
	Mean OD TT	28.4	47.3	16.8	24.2	38.6
ABC	% trip failed	4.2%	6.3%	5.2%	4.1%	7.0%
	Mean OD TT	27.1	47.4	16.1	17.4	37.8
ACB	% trip failed	4.2%	6.3%	2.0%	2.1%	6.5%
	Mean OD TT	26.6	47.3	18.1	23.7	37.7
BAC	% trip failed	4.9%	6.2%	2.1%	2.3%	6.9%
	Mean OD TT	26.9	54	20.9	26.3	39.6
BCA	% trip failed	4.4%	6.2%	4.0%	4.3%	6.5%
	Mean OD TT	26.6	47	29	34	37.1
CAB	% trip failed	4.5%	6.2%	2.0%	2.1%	7.0%
	Mean OD TT	26.6	47.9	15.7	15.6	37.7
CBA	% trip failed	5.2%	6.2%	3.3%	3.3%	6.9%
	Mean OD TT	26.6	46.7	28.2	29.8	37.7

In order to complete the investigation and show that we have multiple equilibria, we need to prove that the solutions do not have similar link flow distributions. To do so, we evaluate the performance of the PT system and the mode choice of users at the equilibrium state. Table 4 presents the usage of PT at the equilibrium state for all scenarios. The number of users who take metro line A is between 2089 and 2983. This means if we open the metro line in the order ACB, we will have 42% more users that take metro line A than in the CAB scenario. This width of interval for metro lines B and C is 1250 and 640. According to the demand scenario, 13530 users have to use the PT system, and other users have the choice between the PT system, driving only or both (combined mode). The other criteria in table 4 show that the different orders of opening the metro lines have an impact on attracting users to use the PT system. In scenario CAB, opening metro line C at the beginning attracts more users to takes this metro line, and then metro line A and after B provides the intermediate solutions which finally converge to an equilibrium with the highest number of users using PT.

Opening metro line A before B when metro line C is activated before the final step always provides a larger number of users using the PT system (e.g., when comparing scenarios CAB and CBA or ACB and BCA). Moreover, the system can manage the use of bus lines and metro lines, e.g., the equilibrium for scenario CBA balances the number of users that use both systems while in other scenarios the share of users who take the bus is larger.

Table 4. Public transportation criteria; (#: number of)

Scenario	Sequence	# of users used Metro			# of users	# of times	# of times	# of times
		A	B	C	used only PT	PT used	metro used	bus used
1	A&B&C	2236	3057	3708	15421	24685	9001	15684
2	ABC	2826	2771	3316	14751	24093	8913	15180
3	ACB	2983	2636	3678	15336	22780	9297	13483
4	BAC	2419	3077	3138	13674	25626	8634	16992
5	BCA	2608	3117	3481	14559	22502	9206	13296
6	CAB	2089	3886	3564	17284	25983	9539	16444
7	CBA	2313	2977	3778	15298	20888	9068	11820

The criteria for the users' choice of mode are presented in table 5 for the equilibrium state of all the scenarios. The results show that we have a different number of users that decide to only drive between their OD pairs, and also a different number of vehicles in the system. Consequently, there are multiple link flow distributions for the end solution of different scenarios, as we expected from the STA case. Choosing the order of opening new metro lines can reduce the number of cars in the system by a maximum of 3%. The combined mode corresponds to the users that start their trip by car and then enter the PT system via a car-park. Scenario CAB, as explained before, motivates more users to use the PT system and also choose a combined mode more than scenario A&B&C in which metro lines are active and empty at the beginning of the experiment. This shows that the intermediate state of the network has a significant impact on the final UE.

Table 5. Mode choice criteria; (#: number of)

Scenario	Sequence	# of users just drive	# of vehicles	Users used Combined mode	Users use PT	Total travel time (hours)
1	A&B&C	34142	39459	9.81%	28.46%	19454.22
2	ABC	36348	40267	7.23%	27.22%	18559.33
3	ACB	36351	40325	7.33%	28.30%	19070.50
4	BAC	37488	40516	5.59%	25.23%	18967.44
5	BCA	37014	40389	6.23%	26.87%	19199.75
6	CAB	33351	39325	11.02%	31.90%	19701.43
7	CBA	36334	40265	7.25%	28.23%	18644.19

The share of users that use the PT system and total travel time are standard criteria for evaluating traffic network performance. According to the results in table 5, by opening the metro lines in the order ABC, we can save 600 hours (3%) on average compared to the other scenarios. The total travel time values of the scenarios are in the range of $[18559.33, 19701.43]$, which is the range of the potential equilibrium space.

Scenario CAB provides a lower number of cars and the highest percentage of PT system use in comparison to the other scenarios. Consequently, the system can choose the specific order for adding new transportation facilities so as to reach equilibrium with appropriate performance with respect to the indicators targeted.

7. Conclusion

In this paper we investigated the impacts of network design history on day-to-day multimodal UE. First, we reviewed studies on the unicity of User Equilibrium (UE) in the urban transportation system. A key argument for unicity is the strictly monotone path travel cost function with respect to the number of travelers that use the path. Generally, in multimodal urban transportation networks, the monotonicity condition simply does not hold. We highlighted the source of multiple equilibria in traffic network systems. A key element is the interactions between modes and the consequences on the travel time. We showed that when such intermediate interactions are stronger than the inter-mode ones, multiple equilibria can be observed. Second, we studied a particular reason for multiple equilibria: network design history. When multiple facilities are progressively introduced in the system at different times, the learning process is subject to multiple steps. When users have time to adjust to these different steps, it changes the global convergence process and may lead the system towards multiple different situations while the final network setting remains the same. In this paper, based on the static and the dynamic context we demonstrated that the order of the successive introduction of such facilities matters when determining the final equilibrium. This is a crucial finding as this means that the study of the current network situation may not be sufficient to grasp the real user distribution inside the network and that it is necessary to consider the history of the network. In other words, a unique UE calculation with the current network setting may lead to an equilibrium other than that resulting from the different steps corresponding to the network history.

Another key result we obtained from the dynamic simulations is that certain final equilibria were more efficient from a systems viewpoint than others. The self-organization of the system led to different network performances depending on the history of the network. The results showed that not only do we have non-unicity, but that total travel time can be saved and other network performance indicators optimized by opening public transportation facilities in a specific order. Consequently, the learning curve is important in a day-to-day DTA model when there is no unicity.

In future work, the authors will build an equilibria prediction model to estimate the multiple possible equilibria of the system and control strategies to shift from one equilibrium to others. Moreover, designing a realistic learning curve is an interesting topic as it can help traffic engineers to predict the equilibrium state. Finally, considering a multi-objective equilibrium or a mixed equilibrium DTA, in this case, is a challenging problem in which the model is closer to the real world. It is also more complex and new sources of non-unicity can be correlated with other components of the system.

Funding

This work was supported by the European Research Council (ERC) under the European Union's Horizon 2020 research and innovation program. (Grant agreement No 646592 – MAGnUM project)

References

Aashtiani, Heayat Zakaie, and Thomas L Magnanti. 1981. "Equilibria on a congested transportation network." *SIAM Journal on Algebraic Discrete Methods* 2 (3): 213–226.

Ameli, M., J. P. Lebacque, and L. Leclercq. 2020. "Cross-comparison of convergence algorithms to solve trip-based dynamic traffic assignment problems." *Computer-Aided Civil and Infrastructure Engineering* 1–22.

Beckmann, Martin, Charles B McGuire, and Christopher B Winsten. 1956. *Studies in the Economics of Transportation*. Technical Report.

Bureau of Public Roads, U.S.A. 1964. *Traffic assignment manual for application with a large, high speed computer*. US Dept. of Commerce, Bureau of Public Roads, Office of Planning, Urban ....

Corman, Francesco, Francesco Viti, and Rudy R Negenborn. 2017. "Equilibrium models in multimodal container transport systems." *Flexible Services and Manufacturing Journal* 29 (1): 125–153.

Dafermos, Stella. 1982. "The general multimodal network equilibrium problem with elastic demand." *Networks* 12 (1): 57–72.

Daganzo, Carlos F. 1985. "The uniqueness of a time-dependent equilibrium distribution of arrivals at a single bottleneck." *Transportation science* 19 (1): 29–37.

Djavadian, Shadi, and Joseph YJ Chow. 2017. "Agent-based day-to-day adjustment process to evaluate dynamic flexible transport service policies." *Transportmetrica B: Transport Dynamics* 5 (3): 281–306.

Florian, Michael, and Donald Hearn. 1995. "Network equilibrium models and algorithms." *Handbooks in Operations Research and Management Science* 8: 485–550.

Florian, Michael, and Calin D Morosan. 2014. "On uniqueness and proportionality in multiclass equilibrium assignment." *Transportation Research Part B: Methodological* 70: 173–185.

Friesz, Terry L, David Bernstein, Z Suo, and Roger L Tobin. 2001. "Dynamic network user equilibrium with state-dependent time lags." *Networks and Spatial Economics* 1 (3-4): 319–347.

Huang, Hai-Jun, and William HK Lam. 2002. "Modeling and solving the dynamic user equilibrium route and departure time choice problem in network with queues." *Transportation Research Part B: Methodological* 36 (3): 253–273.

Iryo, Takamasa. 2011. "Multiple equilibria in a dynamic traffic network." *Transportation Research Part B: Methodological* 45 (6): 867–879.

Iryo, Takamasa. 2013. "Properties of dynamic user equilibrium solution: existence, uniqueness, stability, and robust solution methodology." *Transportmetrica B: Transport Dynamics* 1 (1): 52–67.

Iryo, Takamasa. 2015. "Investigating factors for existence of multiple equilibria in dynamic traffic network." *Networks and Spatial Economics* 15 (3): 599–616.

Iryo, Takamasa, and Michael J Smith. 2018. "On the uniqueness of equilibrated dynamic traffic flow patterns in unidirectional networks." *Transportation Research Part B: Methodological* 117: 757–773.

Iryo, Takamasa, and David Watling. 2019. "Properties of equilibria in transport problems with complex interactions between users." *Transportation Research Part B: Methodological* 126: 87–114.

Janson, Bruce N. 1991. "Dynamic traffic assignment for urban road networks." *Transportation Research Part B: Methodological* 25 (2-3): 143–161.

Jiang, Yu, WY Szeto, Jiancheng Long, and Ke Han. 2016. "Multi-class dynamic traffic assignment with physical queues: intersection-movement-based formulation and paradox." *Transportmetrica A: Transport Science* 12 (10): 878–908.

Jin, Wen-Long. 2007. "A dynamical system model of the traffic assignment problem." *Transportation Research Part B: Methodological* 41 (1): 32–48.

Konishi, Hideo. 2004. "Uniqueness of user equilibrium in transportation networks with heterogeneous commuters." *Transportation science* 38 (3): 315–330.

Krug, Jean, Arthur Burianne, and Ludovic Leclercq. 2019. *Reconstituting demand patterns of the city of Lyon by using multiple GIS data sources*. Technical Report. University of Lyon, ENTPE, LICIT.

Laval, Jorge A, and Ludovic Leclercq. 2008. "Microscopic modeling of the relaxation phe-

nomenon using a macroscopic lane-changing model." *Transportation Research Part B: Methodological* 42 (6): 511–522.

Lebacque, JP, TY Ma, and MM Khoshyaran. 2009. "The cross-entropy field for multi-modal dynamic assignment." *Proceedings of the Traffic and Granular Flow'07* .

Leclercq, Ludovic. 2007a. "Bounded acceleration close to fixed and moving bottlenecks." *Transportation Research Part B: Methodological* 41 (3): 309–319.

Leclercq, Ludovic. 2007b. "Hybrid approaches to the solutions of the "Lighthill–Whitham–Richards" model." *Transportation Research Part B: Methodological* 41 (7): 701–709.

Leclercq, Ludovic, Jorge Andres Laval, and Estelle Chevallier. 2007. "The Lagrangian coordinates and what it means for first order traffic flow models." In *Transportation and Traffic Theory 2007. Papers Selected for Presentation at ISTTT17*, .

Lindsey, Robin. 2004. "Existence, uniqueness, and trip cost function properties of user equilibrium in the bottleneck model with multiple user classes." *Transportation science* 38 (3): 293–314.

Ma, Xiaoyu, Wei Xu, and Caihua Chen. 2021. "A day-to-day dynamic evolution model and pricing scheme with bi-objective user equilibrium." *Transportmetrica B: Transport Dynamics* 9 (1): 283–302.

Marcotte, Patrice, and Laura Wynter. 2004. "A new look at the multiclass network equilibrium problem." *Transportation Science* 38 (3): 282–292.

Mounce, Richard. 2007. "Existence of equilibrium in a continuous dynamic queueing model for traffic networks." In *4th IMA International Conference on Mathematics in TransportInstitute of Mathematics and its Applications*, .

Mounce, Richard, and Mike Smith. 2007. "Uniqueness of equilibrium in steady state and dynamic traffic networks." In *Transportation and Traffic Theory 2007 (ISTTT17).*, .

Nagurney, Anna, and Ding Zhang. 2012. *Projected dynamical systems and variational inequalities with applications*. Vol. 2. Springer Science & Business Media.

Nagurney, Anna B. 1984. "Comparative tests of multimodal traffic equilibrium methods." *Transportation Research Part B: Methodological* 18 (6): 469–485.

Netter, Maurice. 1972. "AFFECTATION DE TRAFIC ET TARIFICATION AU COUT MARGINAL SOCIAL: CRITIQUE DE QUELQUES IDEES ADMISES." *Transp Res* 6 (4).

Nilsson, Gustav, Piyush Grover, and Uroš Kalabić. 2018. "Assignment and Control of Two-Tiered Vehicle Traffic." In *2018 IEEE Conference on Decision and Control (CDC)*, 1023–1028. IEEE.

Osawa, Minoru, Haoran Fu, and Takashi Akamatsu. 2018. "First-best dynamic assignment of commuters with endogenous heterogeneities in a corridor network." *Transportation Research Part B: Methodological* 117: 811–831.

Patriksson, Michael. 2015. *The traffic assignment problem: models and methods*. Courier Dover Publications.

Peeta, Srinivas, and Athanasios K Ziliaskopoulos. 2001. "Foundations of dynamic traffic assignment: The past, the present and the future." *Networks and spatial economics* 1 (3-4): 233–265.

Silva, Hugo E, Robin Lindsey, André De Palma, and Vincent AC Van den Berg. 2016. "On the existence and uniqueness of equilibrium in the bottleneck model with atomic users." *Transportation Science* 51 (3): 863–881.

Smith, MJ. 1983. "An algorithm for solving asymmetric equilibrium problems with a continuous cost-flow function." *Transportation Research Part B: Methodological* 17 (5): 365–371.

Smith, MJ. 1993. "A new dynamic traffic model and the existence and calculation of dynamic user equilibria on congested capacity-constrained road networks." *Transportation Research Part B: Methodological* 27 (1): 49–63.

Smith, Mt J. 1979. "The existence, uniqueness and stability of traffic equilibria." *Transportation Research Part B: Methodological* 13 (4): 295–304.

Sun, Chao, Lin Cheng, and Ting Xu. 2014. "Range of User-Equilibrium Route Flow with Applications." *Procedia-Social and Behavioral Sciences* 138: 86–96.

Wardrop, John Glen. 1952. "ROAD PAPER. SOME THEORETICAL ASPECTS OF ROAD TRAFFIC RESEARCH." *Proceedings of the institution of civil engineers* 1 (3): 325–362.

Wie, Byung-Wook, Roger L Tobin, and Malachy Carey. 2002. "The existence, uniqueness and computation of an arc-based dynamic network user equilibrium formulation." *Transportation Research Part B: Methodological* 36 (10): 897–918.

Wynter, Laura. 2001. *A convergent algorithm for the multimodal traffic equilibrium problem.* Technical Report 4125. Institut National De Recherche en Informatique et en Automatique, Le Chesnay Cedex, France. Available from Internet: https://hal.inria.fr/file/index/docid/72503/filename/RR-4125.pdf.

Yang, Hai, and Hai-Jun Huang. 2004. "The multi-class, multi-criteria traffic network equilibrium and systems optimum problem." *Transportation Research Part B: Methodological* 38 (1): 1–15.

Yang, Hai, and Hai-Jun Huang. 2005. *Mathematical and economic theory of road pricing.*

Zhao, Xiaomei, Chunhua Wan, and Jun Bi. 2018. "Day-to-day assignment models and traffic dynamics under information provision." *Networks and Spatial Economics* 1–30.

Appendix A. Scenario design for the numerical experiment

Table A. The scenarios of network design for the dynamic test case.

	# active metro	Sequence	Scenario	Initial assignment pattern is obtained by (Description)	Optimal assignment path code
Phase 1 (day 0)	0	-	-	All-or-nothing assignment	P1.1
	3	A&B&C	1st Scenario	P1.1 (All metro lines are available for the users)	P1.2
	1	A	-	P1.1 (Just metro A is available)	P1.3
	1	B	-	P1.1 (Just metro B is available)	P1.4
	1	C	-	P1.1 (Just metro C is available)	P1.5
Phase 2 (day 100)	2	AB	-	Phase 1 simulation code P1.3	P2.1
	2	AC	-	Phase 1 simulation code P1.3	P2.2
	2	BA	-	Phase 1 simulation code P1.4	P2.3
	2	BC	-	Phase 1 simulation code P1.4	P2.4
	2	CA	-	Phase 1 simulation code P1.5	P2.5
	2	CB	-	Phase 1 simulation code P1.5	P2.6
Phase 3 (day 200)	3	ABC	2nd Scenario	Phase 2 simulation code P2.1	P3.1
	3	ACB	3rd Scenario	Phase 2 simulation code P2.2	P3.2
	3	BAC	4th Scenario	Phase 2 simulation code P2.3	P3.3
	3	BCA	5th Scenario	Phase 2 simulation code P2.4	P3.4
	3	CAB	6th Scenario	Phase 2 simulation code P2.5	P3.5
	3	CBA	7th Scenario	Phase 2 simulation code P2.6	P3.6